The Hypercycle

A Principle of Natural Self-Organization

Part B: The Abstract Hypercycle

Manfred Eigen
Max-Planck-Institut für biophysikalische Chemie, D-3400 Göttingen

Peter Schuster
Institut für theoretische Chemie und Strahlenchemie der Universität, A-1090 Wien

Topologic methods are used to characterize a particular class of self-replicative reaction networks: the hypercycles. The results show that the properties of hypercycles are sufficient for a stable integration of the information contained in several self-replicative units. Among the catalytic networks studied, hypercyclic organization proves to be a necessary prerequisite for maintaining the stability of information and for promoting its further evolution. The techniques used in this paper, though familiar to mathematicians, are introduced in detail in order to make the logical arguments accessible to the nonmathematician.

V. The Concrete Problem

In Part A of this trilogy on hypercycles we have arrived at some essential conclusions about Darwinian systems at the molecular level, which may be summarized as follows:

1. The target of selection and evolution is the quasispecies, which consists of a distribution of (genotypically) closely related replicative units, centered around the copy (or a degenerate set of copies) corresponding to the phenotype of maximum selective value.
2. The information content of this master copy – expressed as the number ν of symbols (nucleotides) per replicative unit – is limited to $\nu_m < \frac{\ln \sigma_m}{1-\bar{q}_m}$, where $\sigma_m (>1)$ is the superiority of the master copy, i.e., an average selective advantage over the rest of the distribution, and $\bar{q}_m$, the average quality of symbol copying. Exceeding this threshold of information content will cause an error catastrophe, i.e., a disintegration of information due to a steady accumulation of errors.
3. A highly evolved enzymic replication machinery is necessary to reach a stable information content of a few thousand nucleotides. Such an amount would be just sufficient to code for a few protein molecules, as we find in present RNA phages. The physical properties inherent in the nucleic acids allow for a reproducible accumulation of information of no more than 50 to 100 nucleotides.

The last of these three statements may be questioned on the basis of the argument that environmental factors – such as suitable catalytic surfaces or even protein-like enzyme precursors [47] – may cause a considerable shift of those numbers. In fact, the figures given were derived from equilibrium data, namely, from the free energies for (cooperative) complementary versus noncomplementary nucleotide interactions. Nevertheless, we still consider them upper limits which in nature may actually be reached only in the presence of suitable catalysts or via annealing procedures. Laboratory experiments on enzyme-free template-induced polymerization lead to considerably lower numbers. On the other hand, environmental catalysts cannot yield fidelities of symbol recognition exceeding the equilibrium figures, unless they themselves become part of the selectively optimizing system. There is no way of systematically favoring the functionally advantageous over the nonadvantageous interactions, other than via a stepwise selective optimization. The phage genomes could evolve in the form of single-stranded RNA molecules, only because a quite advanced replication and translation machinery was provided by the host cell. They are postcellular rather than precellular evolution products. Something like the magnitude of the information content of their genomes is just what would be required at the beginning of translation, namely, the reproducible information for a set of enzymes that could start a primitive translation mechanism. Hence the essential conclusion from Part A is:

The start of translation requires an integration of several replicative units into a cooperative system, in order to provide a sufficient amount of information for the build-up of a translation and replication machinery. Only such an integrated machinery can bring about a further increase of fidelity and hence allow for a corresponding expansion of the information content.

How can one envisage an integration of competitive molecules, other than by ligation to one large replicative unit, which is prohibitive due to the threshold relation for ν_{max}. (Note that the units to be integrated have to remain competitive with respect to their mutants in order to evolve further and not to lose their specific information.) Let us briefly investigate three possible choices:

1. *Coexistence.* Stable mutual tolerance of self-replicative units in the absence of stabilizing interactions is possible only for individuals belonging to the same quasi-species. The quasi-species distribution could well provide favorable starting conditions for the evolution of a cooperative system. However, it does not favor the evolution of functional features. The coupling stabilizing the quasi-species is solely dictated by the genotypic kinship relations, which usually do not coincide with functional needs. Required is a set of selectively equivalent genotypes that complement each other at the *phenotypic* level. The quasi-species distributions as such does not meet these selection criteria.

2. *Compartmentation.* Enclosure of a Darwinian system in a compartment will not provide a solution of this problem either. The main consequence of compartmentation is an enhancement of competition due to the restriction of living space and metabolic supply. Hence a compartment will only stabilize further a given selectively advantageous quasi-species; it will not favor the evolution of equivalent partners according to functional criteria, which requires the cooperating partners to diverge genotypically. A compartment, however, may offer advantages for a system that has already established a stable cooperation via functional linkages (cf. Part C). More sophisticated compartments such as present living cells, which comprise only one (or a few) copies of each replicative subunit together with a machinery for reproduction of the whole compartment require, of course, a symbol quality $\bar{q}_m$ which is adapted to the total information content according to the relationship for ν_{max}. In other words: They are subject to the same limitations as a fully ligated unit.

3. *Functional linkages.* Selection of functionally cooperating partners may be effected via the functional linkages, which provide either a mutual catalytic enhancement of reproduction or a structural stabilization. A closer inspection of such linkages is the main topic of this paper.

Let us aid our intuition again by playing another version of the computer game introduced in Part A. In the first part of the game the objective was to demonstrate the need for adapting the symbol-reproduction quality to the information content of the sentence to be reproduced. In the second part we assume now that the average quality factor $\bar{q}_m$ is not sufficient for a stable reproduction of the whole sentence in the form of a replicative unit, but suffices for copying units as small as single words. It refers to a natural situation in early evolution, where the physical forces inherent in the nucleotides may have been sufficient for an evolution of stable t-RNA-like molecules (=single words), but did not admit the build-up of an – even primitive – translation apparatus (=a whole 'meaningful' sentence). Accordingly, the computer is programmed just to reproduce single words using error rates sufficient to guarantee their stability against accumulation of errors.

As a first variant of the game let us try to establish a plain coexistence of the four words. For this purpose we attribute to all correct *words* in the sentence the same selective value, while a mistake in any word is of disadvantage with respect to the correct word by a given factor (per bit). As before, the words are allowed to reproduce, the total number being limited to N copies. This variant, however, differs from the original game in that the individual words now behave as independent replicative units. Table 5 shows some typical results: Despite the fact that all words have the same selective value and are able to compete favorably with their error copies, the sentence as a whole is unstable. Only one of the four words can win the competition, but it cannot be predicted by any means which of the four words actually wins. One may characterize this situation by the tautology: 'survival of the survivor'. The term 'fittest' means nothing but the mere result of the contest.

In the next variant of the game we introduce a functional linkage between related words: A given word provides catalytic help for the reproduction of the next word whenever it forms a meaningful sequence:

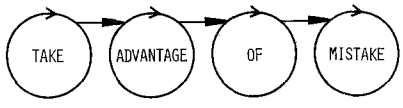

The coupling is proportional to the population number of the catalyst (i.e., to the representation of the particular word in the computer store). In other words, reproduction is facilitated according to a rate law:

$k_1 x_1$ and

$k_i x_i + k_i' x_i x_{i-1}$ for $i = 2, 3, 4$

Naturwissenschaften 65, 7–41 (1978)

Table 5. A game representing the competition of selectively equivalent replicative units

The aim of this game is to preserve the information of the sentence:

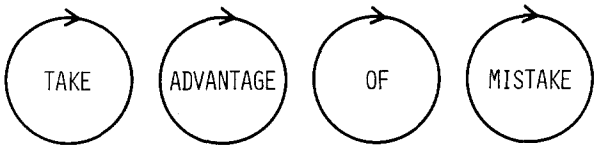

Each word symbolizes a replicative unit. All words have exactly the same selective value. The selective advantage per bit is 2.7. Each letter consists of 5 binary digits.

	Digit mutation probability $(1-\bar{q})$ [%]	Digit number ν	Word quality factor $Q=q^{\nu}$	Error expectation value ε
TAKE	3.15	20	0.53	0.63
ADVANTAGE	1.4	45	0.53	0.63
OF	6.3	10	0.53	0.63
MISTAKE	1.8	35	0.53	0.63

Since there is no coupling among the words every game ends with the *selection of one word.* All words are degenerate with respect to their selective values; therefore, each of the four words has an equal chance to be the survivor. Due to the high *average* error probability ($\sim 2\%$ per bit) the sentence as a whole (125 bits) is not a stable replicative unit.

Below typical results of ten games are listed. The 'X' indicates which word is selected, while all the others die out. The number denotes the generation after which selection is complete.

Game	TAKE	ADVANTAGE	OF	MISTAKE	Generation
1	X				12
2			X		15
3		X			19
4		X			23
5	X				10
6				X	20
7			X		9
8		X			13
9			X		22
10		X			26

Error distribution of the selected word ADVANTAGE. The solid line resembles the Poisson distribution $\frac{\varepsilon^k e^{-\varepsilon}}{k}$; where $\varepsilon=\nu(1-\bar{q})$ is the expectation value for an error in the word ($\nu=45$ bits).
(The errors refer to one single digit. All wrong letters differ from the correct ones in only one of their five digits.)

0 errors	1 error	2 errors	3 errors
ADVANTAGE			
ADVANTAGE			
ADVANTAGE			
ADVANTAGE	ADVANTAG!		
ADVANTAGE	ADVANDAGE		
ADVANTAGE	ADVARTAGE		
ADVANTAGE	ADVINTAGE		
ADVANTAGE	ADFANTAGE		
ADVANTAGE	ADZANTAGE		
ADVANTAGE	AHVANTAGE		
ADVANTAGE	AHVANTAGE	ADVANDACE	
ADVANTAGE	AHVANTAGE	ADVANDAIE	
ADVANTAGE	AFVANTAGE	ADVARXAGE	
ADVANTAGE	AFVANTAGE	ADVINTBGE	ITVANTAGU

x_i or x_{i-1}, resp. being population numbers, in this case referring to the words in the computer store. The result of this game variant is usually fixation of the last word of the sentence, i.e., 'mistake', while all other words die out. Only if the coupling is relatively weak and a particular k_i value is chosen large enough do we find that the corresponding word (i) may outgrow the others, representing selection among (essentially) independent competitors. The result that the last word in the sequence receives all the benefit of coupling (whenever the coupling terms are predominant) may be astonishing. One would expect that there must at least exist a range of stability for the whole sentence. This is certainly true for a certain magnitude of the population numbers, if the values of the rate parameters obey a certain order with respect to the position of the words in the sequence. However, fixed-point analysis as carried out in Section VII will show that, even under those special conditions, only the last member in the chain will grow in proportion to the total population, while all other members assume essentially constant population numbers, irrespective of the size of the total population. Hence, in a growing population, the relative abundance of the last member changes drastically until the system again reaches a range where only the abundant member remains stable. In the process of molecular evolution population numbers of individuals usually show those drastic changes, e.g., from one single mutant up to a detectable magnitude of (more than) billions of copies. Thus the result obtained in our game turns out to be quite representative of what actually would happen in nature.

The fact that linear coupling – if it works at all – feeds all the advantage forward to the last member in the sequence provides a strong hint for a possible solution of the problem: The couplings should form a closed loop:

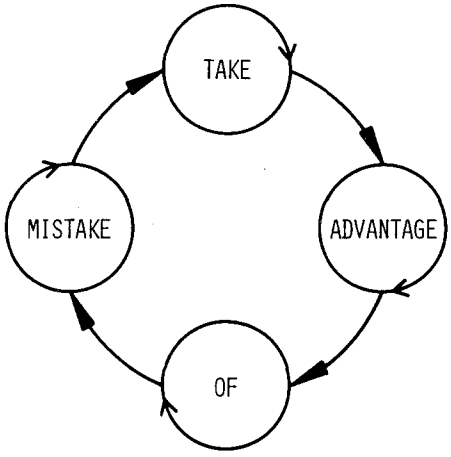

Then the enhancement due to coupling will cyclically fluctuate through all words of the sequence. Our sentence actually was chosen as to provide automatically such a cyclic overlap through the word 'mis*take*'. Since each word is a catalytic cycle (i.e., a self-replicative unit) the system represents a hypercycle of second degree according to our definitions introduced in Part A. The result of the game is represented in Figure 16. All four words show a stable steady-state representation with a periodic variation of their population numbers. The selective values of different words do not have to be the same – which would seem very improbable for any realistic system. Each word, furthermore, is represented by a stable distribution of mutants. Unless one of the words is wiped out by a fluctuation catastrophe (which becomes very improbable at a sufficiently large number of copies) the population numbers will continue to oscillate. In other words: The information of the whole sentence is stable.

VI. General Classification of Dynamic Systems

VI.1. Definitions

In the following sections we shall carry out a more rigorous mathematical analysis of dynamic systems, especially of those which are of importance in precellular self-organization. To determine which systems are relevant we shall have to inspect different classes of reaction networks including both noncyclic and cyclic. Evolutionary processes can be described phenomenologically by systems of differential equations, as has been shown for a particular case in Part A. The term dynamical system then refers to the complete manifold of solution curves of a given set of differential equations.

Let us consider a general dynamic system that is described by n ordinary, first-order, and autonomous differential equations;

$$\frac{dx_i}{dt} \equiv \dot{x}_i = A_i(x_1 \ldots x_n, k_1 \ldots k_m; B); \qquad i = 1, 2, \ldots, n \quad (30)$$

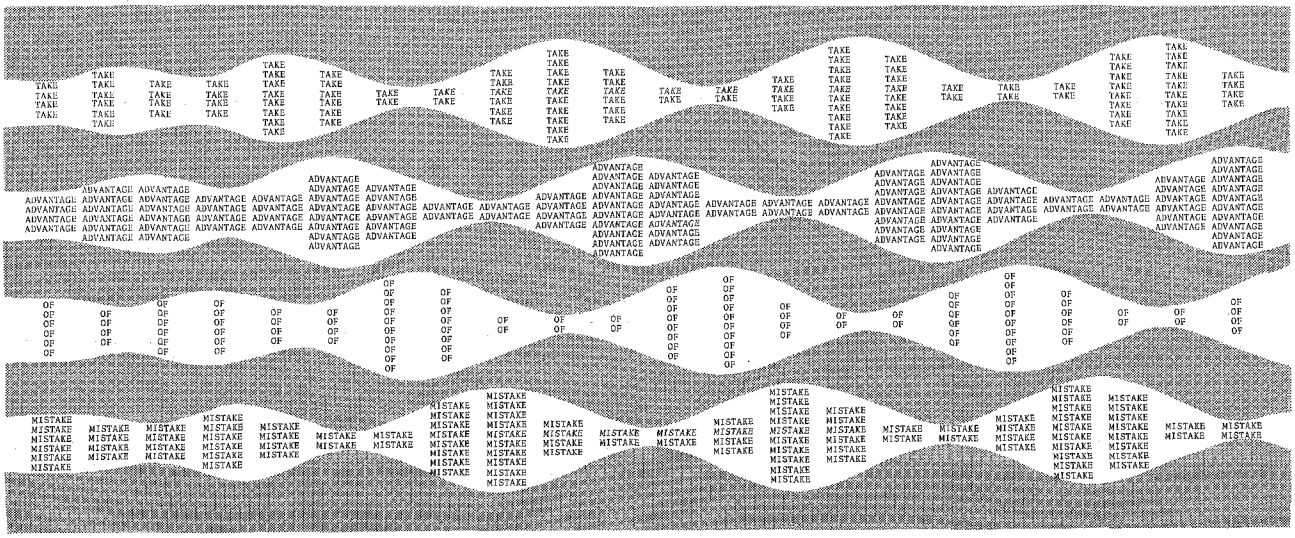

Fig. 16. Each word of the sentence TAKE ADVANTAGE OF MISTAKE represents a self-reproducing unit. The information of the sentence is stabilized by hypercyclic coupling among the words. In the graph, each printed word is representative of 10 copies in the computer store. All words in a vertical row refer to the same time, the intervals of which change discontinuously along the horizontal axis. The oscillation builds up from an initial equipartition of words and maintains a phase shift from word to word. The error distribution for each of the four words is stable and of the same kind as shown in Table 5

Later on we shall extend our analysis also to some nonautonomous systems for which $\Lambda_i = \Lambda_i(t)$.

As before, the x_i represent population variables that usually will refer to self-replicating macromolecular assemblies. The constants $k_i (i = 1, 2, \ldots, m)$ enter as parameters and may be composed of rate constants of elementary processes, of equilibrium constants for reversible and rapidly established reaction steps and of concentrations of those molecules that serve as the (energy-rich) building material for the synthesis of the macromolecules, assuming that these concentrations are buffered and hence can be included as time-independent values. Both the sets of x and k values can be represented as column vectors in a concentration space, or in a parameter space, respectively,

$$\mathbf{x} = \begin{pmatrix} x_1 \\ x_2 \\ \vdots \\ x_n \end{pmatrix} \quad \text{and} \quad \mathbf{k} = \begin{pmatrix} k_1 \\ k_2 \\ \vdots \\ k_m \end{pmatrix}$$

By B we denote the initial conditions for a given set of solution curves, which in our case are represented by the set of initial concentrations $\mathbf{x}_0$.

According to the procedure employed in part A we split the functions Λ_i into three terms:

$$\Lambda_i = \mathrm{A}_i - \Delta_i - \phi_i \tag{31}$$

The A_is comprise all positive contributions to the chemical rate, representing an 'amplification' of the x_i variables, while the Δ_is include all negative rate terms resembling 'decomposition' of the macromolecular species. ϕ_i finally refers to a flux which may effect either dilution or buffering of the component i, depending on the external constraints applied to the system. The difference $\mathrm{A}_i - \Delta_i$ may be called a net growth function Γ_i. Referring to the Darwinian system (cf. part A), Γ_i, in particular, is given by $W_{ii}x_i + \sum_{k \neq i} w_{ik}x_k$, and if summed over all species $k = 1$ to n, it resembles the excess growth function $E = \sum_{k=1}^{n} E_k x_k$.

VI.2. Unlimited Growth

Removal of selection constraints leads to a new system of differential equations

$$\dot{x}_i = \Gamma_i(\mathbf{x}, \mathbf{k}, B) \tag{32}$$

describing a situation which in the following is called 'unlimited growth'. This terminology is representative for the system as a whole; for individual members it may also include decay or stationary behavior.

Assume we can express Γ_i as a polynomial in the various concentrations x_i (which as an approximation may also apply to irrational expressions or ratios of polynomials), then it will usually be possible to find leading terms in Γ_i, which dominate in certain ranges of concentration. These leading terms usually are simple monomials of a given power of x_i. As such they determine the dynamic behavior of the system.

The simple case $\dot{x} = kx^p$ is illustrated in Figure 17. The textbook solutions have been normalized to $x(0) = 1$ and $\dot{x}(0) = 1$. As outlined in the Figure's legend, the whole family of solution curves can be subdivided into three classes, which are restricted to different regions of the concentration/time diagram. Let us consider three representative examples, which will be of particular interest in our forthcoming discussion (cf. Table 6).

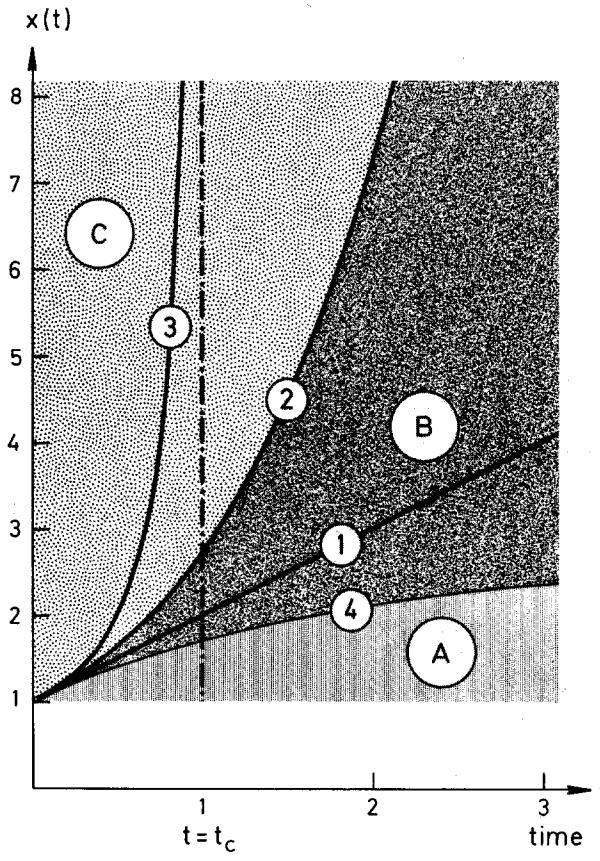

Fig. 17. Different categories of growth can be related to single-term growth functions $\Gamma(x) = \mathrm{d}x/\mathrm{d}t$ (normalized to $\Gamma = 1$ and $x = 1$ for $t = 0$). *Region A* does not include any growth function which could be represented by a simple monomial $\Gamma = x^p$. In this region all population numbers $x(t)$ remain finite at infinite time. The borderline between region A and B is given by the growth function $\Gamma(x) = e^{1-x}$ (curve 4). *Region B* is spanned by all monomials $\Gamma(x) = x^p$ with $-\infty < p < 1$. Curve 1 in this region exemplifies constant growth rate ($p = 0$) equivalent to linear growth. Exponential growth ($p = 1$) provides the borderline between regions B and C (curve 2). While population numbers in region B reach infinity only after infinite time, they show singularities at finite times in region C. As an example, hyperbolic growth ($p = 2$, singularity at $t = t_c = 1$) is shown by curve 3

i) Solution curve **1** represents a system with constant (positive) growth rate. The population variable $x(t)$ increases linearly with time. The solution curve also represents an example for the family of curves in region **B** of Figure 17, which grow to infinity at infinite time. An irreversible formation reaction with totally buffered concentrations of reactants may serve as the most common example. Self-reproducing species in ecologic niches, feeding on independent sources, may adjust their growth rates to the constant influx or production rate of food and then constitute another example for a growth behavior which is independent of the population size.

ii) Solution curve **2** results from growth rates linear in the population variable and exhibits an exponential increase of x with t, typical of Darwinian behavior, as was shown in Part A. The curve **2** furthermore establishes the borderline between regions **B** and **C**, i.e., between functions that reach infinity at infinite and at finite time.

iii) Solution curve **3** finally represents an example for functions with a singularity at finite time $[t_c=(kx_0)^{-1}]$. In this particular case, the growth rate was assumed to be proportional to the square of the population variable.

The whole range **C** may be characterized as 'hyperbolic growth'. Of course, in any real and finite world a population can never grow to infinity, because the available resources are finite and hence constraints will always take care of growth limitations. The phenomena giving rise to the hypothetical existence of a singularity will still cause a behavior quite different from that encountered in Darwinian systems.

At this point we may define the 'degree' p of the growth functions in a more general way, which will turn out to be useful for classification. As before, p_i is the power of the leading term in the growth function Γ_i. An n-dimensional dynamic system then may be characterized by a set of p_i values: $(p_1\, p_2 \ldots p_n)$. When we have a uniform distribution of powers p_i,

$$p_i=p_2=\cdots=p_n\equiv p, \tag{33}$$

we shall call the system 'pure'. Otherwise we are dealing with 'mixed' systems, which may be classified by their distributions of p_i values. Obviously, 'pure' systems can be analyzed much more easily than 'mixed' systems.

VI.3. Constrained Growth and Selection

In reality we shall always encounter constraints which provide certain limits for growth. For experimental studies, we must insure reproducible conditions. It is therefore necessary to formalize these conditions and include them in the theoretical treatment.

In irreversible thermodynamics we would prefer selection constraints that facilitate a thermodynamic description, e.g., constant generalized forces or constant generalized fluxes. For the analysis presented here, we have to adjust these to conditions for selection and evolution that can be materialized in nature. The constraints ϕ_i, as used in Equation (31), are too general for any straightforward analysis. In general we may distinguish between specific and nonspecific selection constraints. In the first case, the constraints act specifically on a single species or on a few species whereas the second case refers to regulation of a global flux ϕ. Then changes in all population variables are proportional to their actual values x_i:

$$\phi_i=\frac{x_i}{c}\,\phi \tag{34}$$

In practice, nonspecific selection constraints can be introduced into a dynamic system by the application of a continuous dilution flux. Thereby the total concentration, $c=\sum x_i$, can be controlled. The corresponding differential equation for c:

$$\dot{c}=\sum_{j=1}^{n}\dot{x}_j=\sum_{j=1}^{n}\Gamma_j(\mathbf{x})-\phi \tag{35}$$

fulfils the condition of stationarity: $\dot{c}=0$, when the flux is adjusted to compensate the net excess production:

$$\phi=\phi_0=\sum_{j=1}^{n}\Gamma_j(\mathbf{x}) \tag{36}$$

This selection constraint, referred to as 'constant organization', has been introduced previously and was also used in Part A. Condition (36) will be used frequently in the following sections to facilitate a general analysis of selection processes. Other constraints have been investigated as well [53]. As will be seen in the next section, the important features of selective and evolutive processes are fairly insensitive to the constraints applied. (These, of course, are always reflected in the quantitative results.)

The condition of constant organization leads to the following differential equations for the dynamic system:

$$\dot{x}_i=\Gamma_i(\mathbf{x})-\frac{x_i}{c_0}\sum_{j=1}^{n}\Gamma_j(\mathbf{x}),\qquad i=1,2,\ldots,n \tag{37}$$

Here c_0 denotes the stationary value of the total concentration which may be maintained by regulation of the flux to the value ϕ_0.

The individual selection behavior for the three simple growth functions: $p=0$, 1, and 2, as discussed in connection with Figure 17, is detailed in Table 6:

Table 6. Growth rates and selection behavior under the selection constraints of constant overall organization in the dynamic system $\dot{x}=\Gamma-\phi$

	p	Unlimited growth			Long-term behavior under constraints of constant organization	
		Growth rate $\Gamma(x)$	Solution curve	Type of growth	$\bar{\mathbf{x}}$	Type of selection behavior
1	0	k	$x=x_0+kt$	linear	$\bar{x}_i=k_i c_0/\sum k_j$	Coexistence of species with no selection
2	1	kx	$x=x_0\cdot\exp(kt)$	exponential	$\bar{x}_k=c_0, \bar{x}_i=0$ $k_k-k_i>0, i\neq k$	Competition leading to selection of the globally 'fittest' species
3	2	kx^2	$x=x_0(1-kx_0t)^{-1}$	hyperbolic	$\bar{x}_k=c_0, \bar{x}_i=0$ $k=1,2,\ldots,n; i\neq k$	Competition aiming at local optimization 'once-for-ever' decision

i) Constant growth rates – corresponding to a linear increase of the population with time – yield under the constraint of constant organization a stable coexistence of all partners present in the system. Upgrowth of advantageous mutants shifts the stationarity ratios without causing the total system to become unstable.
ii) Linear growth rates, corresponding to an exponential increase of the population size, result in competition and selection of the 'fittest'. Advantageous mutants, upon appearance, destabilize and replace an established population.
iii) Nonlinear growth rates ($p>1$), characterized by hyperbolic growth, also lead to selection, more sharply than in the Darwinian system mentioned under ii). Mutants with advantageous rate parameters, however, in general will not be able to grow up and destabilize an established population, since the selective value is a function of the population number (e.g., for $p=2$, $W\sim x$). The advantage of any established population with finite x hence is so large that it can hardly be challenged by any single mutant copy. Selection then represents a 'once-for-ever' decision. Coexistence of several species here requires a very special form of cooperative coupling.

The examples mentioned are quite representative. We may classify systems according to their selection behavior as coexistent or competitive. In a given system we may encounter more than one type of behavior.

VI.4. Internal Equilibration in Growing Systems

While the condition of constant organization simplifies the analysis of dynamic system considerably, it is limited to systems with zero net growth. In this section we shall try to extend the range of applicability. The main problem is to find out in which way and under which conditions predictions on growing systems can be made, given the results obtained from an analysis of the corresponding stationary states. For this purpose we introduce nonspecific and time-dependent selection constraints (Eq. 34):

$$\dot{x}_i=\Gamma_i(\mathbf{x})-\frac{x_i}{c(t)}\,\phi(t) \tag{38}$$

Either $c(t)$ or $\phi(t)$ can be chosen freely. The other function, however, is determined then by the following differential or integral equation, respectively.

$$\phi(t)=\sum_{i=1}^{n}\Gamma_i(\mathbf{x})-\frac{\mathrm{d}c}{\mathrm{d}t} \quad \text{or} \tag{39}$$

$$c(t)=c_0+\int_0^t\left\{\sum_{i=1}^{n}\Gamma_i(\mathbf{x})-\phi(\tau)\right\}\mathrm{d}\tau \tag{40}$$

It is appropriate now to introduce normalized population variables $\boldsymbol{\xi}=\frac{1}{c}\,\mathbf{x}$. The differential equations then can be brought into the form:

$$\dot{\xi}_i=\frac{1}{c(t)}\{\Gamma_i(\mathbf{x})-\xi_i\Sigma_j\Gamma_j(\mathbf{x})\} \tag{41}$$

As we see immediately, $\dot{\xi}_i$ does not depend explicitly on the selection constraint $\phi(t)$. There is, however, an implicit dependence through $c(t)$. We therefore push our general analysis one step further by considering some obvious examples: Let us assume that the net growth functions $\Gamma_i(\mathbf{x})$ are homogeneous of degree λ in x. Although this condition seems to be very restrictive we shall see that almost all our important model systems will correspond to it, at least under certain boundary conditions. Homogeneity in x leads to the same condition as the requirement of a defined degree $p(\lambda=p)$ in the unlimited growth system (see Sec. I.5). Now, the transformation of variables is rather trivial:

$$\Gamma_i(\mathbf{x})=\Gamma_i(c\,\boldsymbol{\xi})=c^{\lambda}\Gamma_i(\boldsymbol{\xi}) \tag{42}$$

and we obtain for the rate equation:

$$\dot{\xi}_i=c^{\lambda-1}\left\{\Gamma_i(\boldsymbol{\xi})-\xi_i\sum_{j=1}^{n}\Gamma_j(\boldsymbol{\xi})\right\} \tag{43}$$

Two important conclusions can be drawn from a simple inspection of this equation: If $\lambda=p=1$, i.e., for a

Darwinian system as discussed in Part A, the dependence on c vanishes and not only the long-term behavior but also the solution curves are identical in growing and stationary systems as far as relative population variables ξ_i are concerned.
If $\lambda = p \neq 1$, the long term behavior of ξ will be identical with that for the stationary system at constant organization, provided $c(t)$ becomes neither zero/nor infinite. Thus for all realistic systems with homogeneous net growth functions Γ_i, the results of fixed-point analysis in ξ space, as obtained in the next section, will be valid also for the case of growing populations.
It is possible to generalize the latter result also to other classes of growth functions, as will be shown in the section on fixed-point analysis. Internal equilibration simplifies analysis of complex dynamic systems tremendously. In many cases the results become identical or similar to those for stationary conditions. If we analyze for the selective behavior of a system, these are the conditions which count. In the following section we shall inspect more closely various dynamic systems under these conditions.

VII. Fixed-Point Analysis of Self-Organizing Reaction Networks

VII.1. The Appropriate Method of Analysis

In analyzing various molecular processes of self-organization we are naturally more interested in the final outcome of selection than in a detailed resolution of the dynamic process. Accordingly, in this section we do not need all the information that is provided by the complete set of solution curves satisfying a system of differential equations. Fixed-point analysis, therefore, is our method of choice, because it serves best the purposes of a comparative analysis of selective behavior. Only in some cases shall we also consult more sophisticated techniques, such as the inspection of the complete vector fields.
Nowadays, fixed-point analysis is a routine technique for studying the long-term behavior of dynamic systems. It can be found in mathematical textbooks or treatises (see, e.g., [48]). Fixed-point analysis has also been applied to problems of economics and to ecologic models as well as to chemical reactions far from equilibrium [49]. A summary of the present stage of development was given recently in a progress report [50].

VII.2. Topologic Features

Let us imagine a mountainous country for which we have a map (cf. Fig. 18). The contour lines in the two-dimensional map provide us with a vague feeling for the three-dimensional scenery. It is this kind of problem that fixed-point analysis deals with. The landscape corresponds to a potential surface along which the dynamic system is moving. In most cases a complete knowledge of this potential surface is not required, and therefore a 'fixed-point map' will turn out to be much simpler than a survey map we use to orient ourselves in an unknown region. In general, the 'fixed-point map' shows exclusively the positions of locally highest and lowest points, such as mountain peaks, passes, and valleys, which are called sources, saddles, and sinks. Such special points are the fixed points of the potential field. Often it is necessary to include also the ridges as

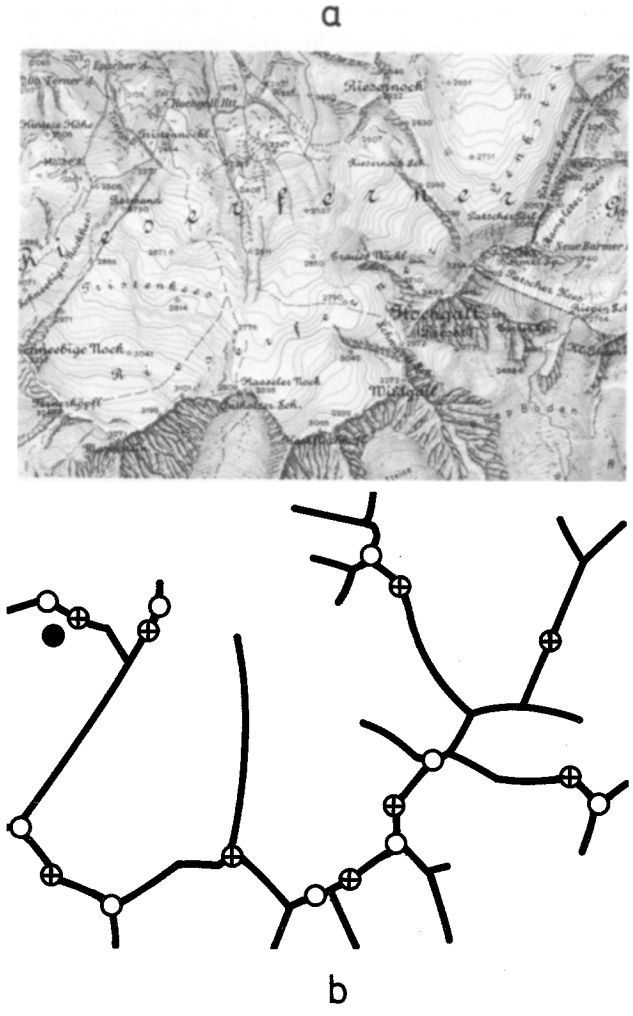

Fig. 18. a) A topographic map provides an abstract representation of a landscape. The lines drawn connect points of equal altitude. The picture shows a region in the Eastern Alps. (reprinted from „Österreichische Karte" 1:50000 Blatt Nr.177 (1962) by courtesy of Bundesamt für Eich- und Vermessungswesen Abt. Landesaufnahme). b) The fixed-point map is a further abstraction of the topographic map. The drawing records the fixed points of a): ○ sources or peaks, ⊕ saddle points, ● sinks; the solid lines here mark the separatices

lines which separate one valley from another (Fig. 18). Characteristically, they are called 'separatrices'. A fixed-point map including separatrices is sufficient to predict where a trajectory starting from a given point on the map will lead. Trajectories are the lines of steepest descent, which in a landscape will be followed by flowing water. The gravitational potential field on the surface of the earth, on the other hand, is less complicated than the fields we encounter in self-organizing dynamic systems. Whereas water flowing on earth always approaches a sink, such as a lake, self-organizing dynamic systems may show a more complex behavior. For instance, there are situations called limit cycles where – in the language of our illustration – water would never stop flowing at a certain point but rather would circulate forever along a closed line determined by the shape of the potential field. Even stranger situations have been described, to which mathematicians actually refer as 'strange attractors', representing something like nonperiodic orbits. Attractor is a more general expression than sink. It includes not only sinks, but also stable closed and nonperiodic orbits.

In a fixed-point map, the whole area under consideration can be separated into a number of regions usually called basins, belonging to individual attractors. The boundaries of these regions are the separatrices. Thus, from all points of a basin the water flows to the same attractor, which of course has to lie inside that region.

Now let us be more precise and characterize the quantities and expressions that are necessary for further discussion in mathematical terms. Fixed points or invariant points of dynamic systems are defined as those points at which all concentrations or population variables, x_i, are constant in time. Hence, the first time derivatives vanish

$$\dot{x}_i = 0, \quad i = 1, 2, \ldots, n \tag{44}$$

thereby determining the positions of all fixed points belonging to a given dynamic system. When all random fluctuations in population variables are strictly suppressed, integration of the dynamic system starting at a fixed point trivially leads to time-independent, constant populations. The response of the system to small changes in concentration at given fixed points provides an excellent tool for a classification of these points. It can be described by a set of normal modes with reciprocal time constants ω_k, which are obtained as the eigenvalues of a system of linear differential equations representing the best fit of the nonlinear system around the point of reference (cf. VII.4). Accordingly we can distinguish four main classes of fixed points.

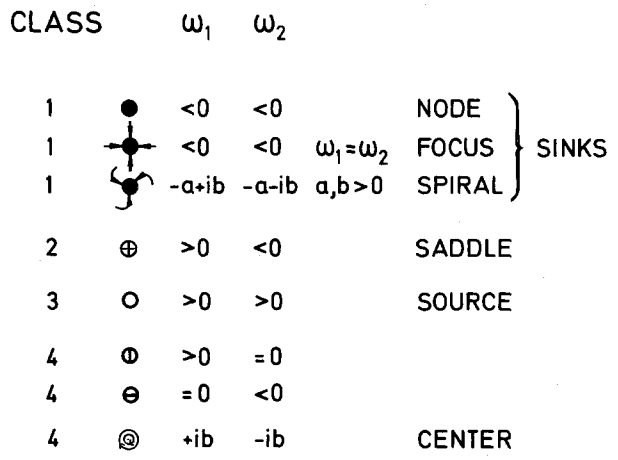

Fig. 19. Symbols are used to classify various fixed points: Class 1: stable fixed points or sinks; Class 2: saddle points; Class 3: sources; Class 4: unstable fixed points including eigenvalues ω with zero real parts. The examples refer to a two-dimensional dynamic system

(1) *Stable fixed points or sinks*, i.e., locally lowest points. All eigenvalues ω_k have negative real parts and hence fluctuations along all possible directions in concentration space are compensated by an internal counteracting force. In chemistry, sinks correspond to chemical equilibria in closed and to stable stationary states in open thermodynamic systems.

(2) *Saddle points* with at least one direction of instability. Here one ω_k value at least will have a positive real part. Consequently, a small perturbation or fluctuation in this direction introduces a force that tends to increase the fluctuation. As a result the dynamic system will move away from the saddle.

(3) *A source* representing a locally highest point. It differs from the saddle only by the fact that it is unstable with respect to *all* directions. All ω_k values have positive real parts.

(4) *Another class of fixed points*, which cannot be analyzed completely within the linear approach. Some of the frequencies ω_k show zero real parts and the nonlinear contributions may change their nature. An example is provided by centers that are defined by purely imaginary eigenvalues, and whose trajectorial representations are manifolds of concentric orbits. We shall encounter such situations in this paper.

After 'long enough' time – which means a period much longer than the largest time constant of the dynamic system – every realistic dynamic system (i.e., a system without external suppression of fluctuations) will approach an attractor. Thus the result of selection will always coincide with an attractor in concentration space.

The final result of a selection process corresponds either to a stable stationary state or to a continuously and periodically changing family of states. In some very rare situations nonperiodic changes within a defined set of states may occur as well. For all these stable or quasi-stable final situations a common, general expression is used in differential topology: the 'attractor' of the dynamic system, which includes the stable point, the closed orbit, and the aperiodic line. Within a given basin, the result of a selection process is approach to an attractor, which is independent of the particular initial conditions.

VII.3. An Appropriate Space: the Concentration Simplex

The concentration variables or population numbers span the n-dimensional open space $\mathbb{R}^n$: $\{x_1, x_2, \ldots, x_n; -\infty < x_i < \infty,\ i=1,2,\ldots,n\}$, only part of which is physically meaningful:

$$\mathbb{X}^n \subset \mathbb{R}^n;\ \mathbb{X}^n: \{x_1, x_2, \ldots, x_n;\ x_i \geqq 0,\ i=1,2,\ldots,n\} \quad (45)$$

All concentration variables can be summed to give a non-negative and finite total concentration c:

$$c = \sum_{i=1}^{n} x_i, \qquad 0 \leqq c < \infty$$

which is used for normalization:

$$\xi_i = \frac{x_i}{c}; \qquad 0 \leqq \xi \leqq 1; \qquad \sum_{i=1}^{n} \xi_i = 1 \quad (46)$$

According to the properties of the variables $\mathbb{X}^n$ can be mapped now isomorphically onto a unit simplex (S_n) for any given value of $c = c_0$. (The corresponding space will be denoted by $\mathbb{S}^n$):

$$c = c_0:\ \mathbb{X}^n \Leftrightarrow \mathbb{S}^n: \{\xi_1, \xi_2, \ldots, \xi_n\} \quad (47)$$

A unit simplex S_n is a regular polyhedron with n corners in the corresponding $(n-1)$-dimensional subspace defined by $\sum_{i=1}^{n} \xi_i = 1$. The edges of a simplex are of unit length and represent coordinate axes for the variables ξ_i. As an illustrative example S_3 is shown in Figure 20. Diagrams on S_3 are familiar to chemists from the representations of ternary systems.

As a consequence of Equation (46) the dynamic system on the unit simplex has lost one degree of freedom compared to $\mathbb{X}^n$. In other words: Due to normalization, the variables ξ_i always refer to a fixed value of $c = c_0$ and thereby one linear dependence is introduced among the variables.

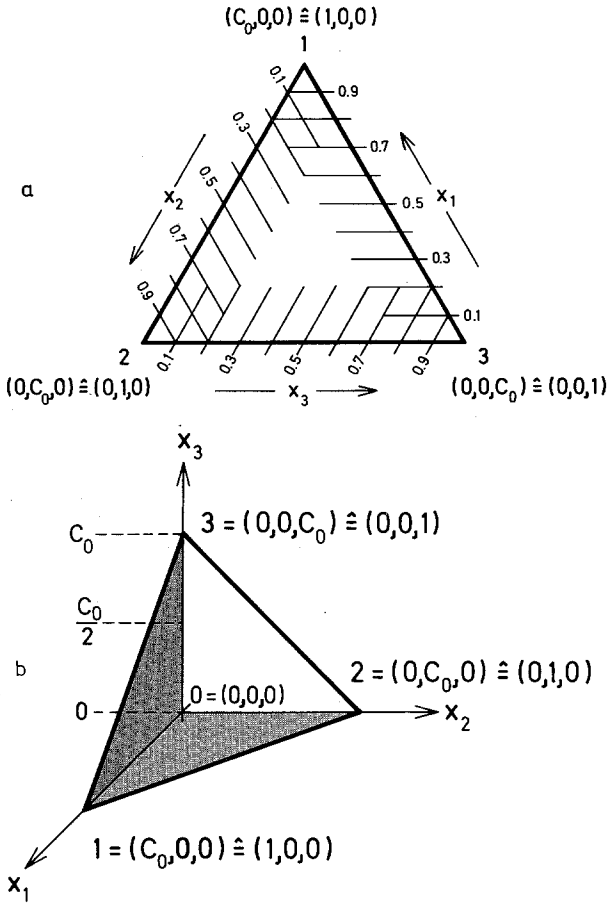

Fig. 20. Diagram a) illustrates the simplex S_3 while diagram b) shows how it is embedded in the physically accessible concentration space. For some of the points the total concentrations $c_0 = \sum_i x_i$, or the coordinates x_1, x_2, x_3 and ξ_1, ξ_2, ξ_3 are given in parenthesis

Finally, we would like to stress a difference between maps on $\mathbb{X}^n$ and $\mathbb{S}^n$ which becomes apparent when we compare results obtained for different values of c_0. Due to normalization, the size of the simplex S_n is fixed, whereas the physically accessible region of $\mathbb{X}^n$ varies with c_0. The positions and the normal modes of fixed points, in general, will depend on c_0 too. For a complete description of the long-term behavior of dynamic systems, it is necessary to evaluate fixed-point maps which themselves are 'functions' of the total concentration c_0. Many fixed points, as we shall see later, show a simple concentration dependence: Their coordinates are proportional to c_0. Upon changes of the total concentration c_0, these points move along lines passing through the origin of $\mathbb{X}^n$ (see Fig. 21) and consequently are mapped as single points on S_n. Accordingly the fixed-point map as a whole becomes much simpler. This formal dependence of fixed-point maps on the values of total concentration c_0 will be of particular importance in the analysis of growing systems.

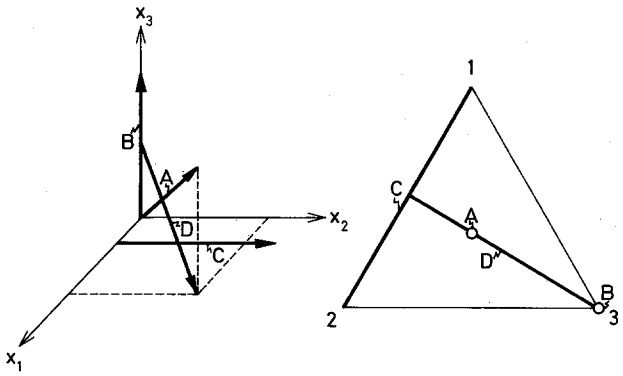

Fig. 21. Illustration of some points with positions exhibiting characteristic dependence on total concentration c_0 in concentration space $\mathbb{X}_3$ (a) and on the simplex S_3 (b). $\mathbf{A}=(c_0/3, c_0/3, c_0/3)$, $\mathbf{B}=(0, 0, c_0)$, $\mathbf{C}=(1, c_0-1, 0)$ and $\mathbf{D}=(c_0-1, c_0-1, 2-c_0)$. The arrows in a) indicate where the points migrate with increasing total concentration (note that those points for which all coordinates are proportional to c_0 like **A** and **B** are mapped into single points on S_3)

A highly symmetric part of a particular $(n-1)$-dimensional hyperplane embedded in n-dimensional concentration space is called the unit simplex. An illustration of a simplex, which can be described in three-dimensional space and therefore is easy to visualize, is given in Figure 20. The unit simplex includes the total physically meaningful range of concentrations and is best suited for a diagrammatic representation of selective processes.

VII.4. Normal Mode Analysis

Starting from the general system of nonlinear differential equations we first determine the fixed points according to $\dot{x}_i=0$. For a straightforward analysis of a dynamic system, it is important to know *all* the fixed points in the region under investigation. In general, however, this information will not be sufficient. Trajectories of the n-dimensional dynamic system will often end in sinks. However, there may be stable closed orbits or strange attractors, the existence of which can be guessed by a careful inspection of the nature of the fixed points in the surrounding region and an analysis of the vector fields. For instance, stable limit cycles in two dimensions can be identified by Poincaré maps. Information on the nature of the fixed points can be obtained by normal mode analysis.

For this purpose the dynamic system is linearized in the neighborhood of a given fixed point $\bar{\mathbf{x}}$:

$$\dot{z}_i=A_i(\bar{\mathbf{x}})+\sum_{j=1}^{n} A_{ij}z_j+O(|\mathbf{z}|^2) \tag{48}$$

The new variables z_i are defined by

$$z_i=x_i-\bar{x}_i \quad \text{or} \quad \mathbf{z}=\mathbf{x}-\bar{\mathbf{x}} \tag{49}$$

while the coefficients A_{ij} are the elements of an $n\times n$ Jacobian matrix (**A**) defined at the fixed point $\bar{\mathbf{x}}$:

$$A_{ij}=\left(\frac{\partial A_i}{\partial x_j}\right)_{\mathbf{x}=\bar{\mathbf{x}}} \tag{50}$$

Since $A_i(\bar{\mathbf{x}})=0$ by definition of the fixed point, the linearized system of differential equations is given by

$$\dot{\mathbf{z}}=\mathbf{A}\cdot\mathbf{z} \tag{51}$$

The reciprocal time constants referring to the normal modes are obtained now as eigenvalues of the matrix **A**. The eigenvectors ξ_i determine the corresponding linear combinations of concentration variables.

$$\mathbf{A}\cdot\zeta_j=\omega_j\cdot\zeta_j \tag{52}$$

The ω_j, in general, are complex quantities and determine the nature of the fixed points, the most important ones of which have been summarized already in Figure 19.

Provided the matrix **A** is not singular, a stable fixed point of the linearized system (51) corresponds to a stable fixed point of the nonlinear problem in almost all cases [51]. There are, however, some important exceptions ($\mathrm{Re}\,\omega_j=0$): A center in the linear system may appear as a spiral sink in the nonlinear case and *vice versa*. The famous Lotka-Volterra model system represents one example for this kind of behavior [52]. We shall encounter another one, the hypercycle of dimension $n=4$, in Section VIII.1.

If more than one stable fixed point, limit cycle, or other attractor is obtained for a given dynamic system, we would also like to know the basins for which the attractors represent the infinite time limits of the trajectories. Individual basins are separated by separatrices, which can be determined in principle by backward integration ($t\rightarrow -t$) starting from saddle points and following the lines of steepest descent. If all stable fixed points and other attractors for a given dynamic system as well as their basins are known, we can predict the result of a selection process starting from any point in the given concentration space.

In some cases we shall obtain $\mathrm{Re}\,\omega_j=0$. Linearization around the fixed point then does not provide enough information, and one has to go back to the nonlinear dynamic system for a complete characterization. Often, direct inspection of the vector field around the fixed point is not too involved and yields the desired results.

Determination of normal modes is an intrinsic part of fixed-point analysis. It represents an inspection of the trajectories of the dynamic system in the close vicinity of the fixed point. In most cases it is sufficient to characterize the stability properties of the fixed point. The linear approximations involved, however, may not always suffice to provide enough information, requiring more sophisticated methods of analysis.

VII.5. Growing Systems

From Equation (37) it is easy to deduce a differential equation for the total concentration c:

$$\dot{c}=\sum_{j=1}^{n} f_j(\mathbf{x})\left(1-\frac{c}{c_0}\right) \tag{53}$$

c_0 represents the stationary value of the total concentration which is controlled by the unspecific flux ϕ_0.

Apparently, this equation has a fixed point at $c=c_0$. The eigenvalue of the normal mode

$$\omega_c = -\frac{1}{c_0}\left(\sum_{j=1}^{n} \Gamma_j(\mathbf{x})\right)_{c=c_0} \tag{54}$$

is negative as long as the sum of all net growth terms Γ_i is positive. Thus we find a stable stationary state at $c=c_0$.

In certain systems the fixed-point maps referring to internal organization also depend on the values of the total concentrations c_0. Now, we are in a position to attribute some physical meaning to the former purely mathematical treatment. For this purpose we assume a nonstationary dynamic system, which starts to evolve at $t=t_0$ with a corresponding initial value of total concentration, $c(t_0)=c_0$. Selection constraints will be adjusted in such a way that the total concentration $c(t)$ changes slowly in comparison to the internal processes of the dynamic system, i.e., all changes due to external processes are much slower than changes due to internal organization. The system approaches a stable solution (i.e., a sink, a stable closed orbit or another kind of attractor) at every instant. When the preceding conditions are fulfilled the system comes closely enough to the long-term solution and the time-dependent process can be described as a sequence of stationary solutions with continuously changing total concentration. In more physical terms we may say, the dynamic system develops under established internal equilibrium. As expected, the analysis of a system can be simplified enormously if the condition of internal equilibration is fulfilled.

Internal equilibration in dynamic systems with *homogeneous* growth functions Γ_i is easy to analyze, because in this case the fixed-point maps S_n do not depend on the total concentrations c_0. From low to high values of c_0 no change in the selective behavior will occur. Moreover, in growing homogeneous system the long-term development does not depend on the degree of internal equilibration. The ultimate result of a selection process, thus, will be the same in systems of this type, independent of whether internal equilibrium has been established during the growth period or not. There are, however, situations to which the concept of internal equilibration must not be applied without careful analysis. At certain critical total concentrations, $c=c_{cr}$, discontinuous changes may occur in fixed-point maps, e.g., sinks may become unstable, stable limit cycles may disappear, etc. A well-known instability of this kind is represented by a 'Hopf bifurcation' [58]. An internally equilibrated dynamic system which reaches such a point from one side, e.g., a growing system approaching the critical concentration from lower values, is essentially off equilibrium after it passes the critical point. For the analysis of dynamic systems in the surroundings of such points, special care is needed. We shall encounter some such examples in Section VII. A very general study of similar situations has been pursued by R. Thom [59] in his catastrophe theory.

These complicated dynamic systems, of course, are more interesting from the biophysical point of view. In fact, the emergence of organized structures requires drastic changes like the discontinuities mentioned above in the fixed-point maps. Inevitably, dynamic systems describing transitions between different levels of organization have to pass through certain critical stages or periods. To be more concrete we shall consider one example representing an important problem in self-organization of biologic macromolecules: the transition from independent competitors to a functional unit consisting of cooperating polynucleotides and proteins. According to the definition given in Section I.4, only one species is selected in a competitive system and hence there is no stable attractor in the interior of S_n. Any cooperative system, on the other hand, has to have such an attractor, otherwise at least one of the cooperating macromolecules would die out after long enough time. Consequently, a dynamic system, which in principle is able to simulate the desired development from a more random to a more organized state, must contain a critical instability at certain values of its parameters.

VII.6. Analysis of Concrete Systems

a) Independent Competitors

As a lucid example for the application of the method of fixed-point analysis we consider the problem of selection of a quasi-species, treated in Part A. The mathematical framework is compiled in Table 7. The coordinates of the concentration space are given by the normal variables y_k; the eigenvalues λ_k are the growth parameters of the functions Γ_k. The analysis refers to a given distribution of mutants. Appearance of new mutants that provide any contribution to the selected quasi-species will change the meaning of the concentration coordinates y_k, i.e., their correlations with the true concentration variables x_k. The results in Table 7 are self-explanatory. We shall use them in the following for a comparative discussion of the three growth functions $\Gamma_i = k_i x_i^p$ which appear in Table 6, i.e.:

1. Constant growth rate: $p=0$
2. Linear growth rate: $p=1$
3. Quadratic growth rate: $p=2$

1. The first case yields one stable fixed point, a focal sink inside the unit simplex S_n:

$$\bar{\mathbf{x}} = \frac{c_0}{\sum_{j=1}^{n} k_j}\begin{pmatrix} k_1 \\ k_2 \\ \vdots \\ k_n \end{pmatrix} \tag{55}$$

'Inside' the unit simplex means for all coordinates of $\bar{\mathbf{x}}$: $0<\bar{x}_i<c_0$. The (negative) eigenvalue of the Jacobian matrix is n-fold degenerate

$$\omega = -\frac{\sum_{j=1}^{n} k_j}{c_0} \tag{56}$$

holding also for ω_c, which refers to the variation of the total concentration c.

The result is stable coexistence of all species.

2. The second case is treated in Table 7. As we recall there is only one stable fixed point. The fact that it is situated at the corner of the simplex indicates competitive behavior. Only one of the concentration coordinates of the nodal sink is positive ($=c_0$), all others being zero. As in the first case, the map does not depend on the overall concentration c_0, nor is the final result dependent on initial conditions.

Table 7. Fixed-point analysis of the selection of a quasi-species (cf. part A)

The rate equation reads:

$$\dot{y}_i = \lambda_i y_i - \frac{y_i}{c_0}\sum_{j=1}^{n}\lambda_j y_j; \qquad i=1,2,\ldots,n.$$

The long-term behavior is determined by n fixed points at the corners of the simplex S_n

$$\bar{\mathbf{y}}_1 = \begin{pmatrix} c_0 \\ 0 \\ \vdots \\ 0 \end{pmatrix} \quad \bar{\mathbf{y}}_2 = \begin{pmatrix} 0 \\ c_0 \\ \vdots \\ 0 \end{pmatrix} \quad \cdots \quad \bar{\mathbf{y}}_n = \begin{pmatrix} 0 \\ 0 \\ \vdots \\ c_0 \end{pmatrix}$$

Normal mode analysis yields for every fixed point $\bar{\mathbf{y}}_k$ a spectrum of n $\omega_j^{(k)}$ values.

$$\begin{array}{llll} \omega_j^{(1)} = \lambda_j - \lambda_1 & \omega_j^{(2)} = \lambda_j - \lambda_2 & \cdots & \omega_j^{(n)} = \lambda_j - \lambda_n \\ j = 2,3,\ldots,n-1,n & j = 1,3,\ldots,n-1,n & & j = 1,2,\ldots,n-2,n-1 \\ \omega_c^{(1)} = -\lambda_1 & \omega_c^{(2)} = -\lambda_2 & & \omega_c^{(n)} = -\lambda_n \end{array}$$

With respect to the degrees of freedom of the simplex S_n, each fixed point $\bar{\mathbf{y}}_k$ has $n-1$ normal modes with the reciprocal time constants $\omega_j^{(k)}$ describing the process of internal organization of the distribution resulting from competition among different quasi-species. Furthermore the simplex S_n has one normal mode $\omega_c^{(k)}$ which corresponds to a variation of the total concentration c. All internal modes $\omega_j^{(k)}$ are represented by differences of eigenvalues λ. Hence there is only one stable fixed point for the largest eigenvalue: $\lambda_m > \lambda_j$, $j=1,2,\ldots,n$, $j \neq m$. It is a nodal sink, i.e., all $\omega_j^{(m)}$ values are different and negative. Accordingly, the quasi-species with the smallest eigenvalue is described by a source, owing to its positive ω_j values. The remaining $n-2$ fixed points then are saddle points, because they involve positive as well as negative normal-mode rate constants $\omega_j^{(k)}$.

3. The third case finally shows a total of 2^n-1 fixed points, which can be grouped in three classes.
The first class includes n focal sinks, one at each of the corners of S_n

$$\bar{\mathbf{x}} = \begin{pmatrix} 0 \\ \vdots \\ x_k = c_0 \\ \vdots \\ 0 \end{pmatrix} \quad \text{with} \quad \begin{array}{l} \omega_j^{(k)} = -k_k c_0 \quad j=1,2,\ldots,n-1 \\ \omega_c^{(k)} = -k_k c_0 \end{array} \qquad (57)$$

These are the only stable fixed points. Being at the corners of the unit simplex they indicate again a competitive behavior, allowing for only one survivor, i.e., a pure state. In this case of nonlinear growth rates, however, the result of the competition depends on initial conditions, since there are n stable fixed points (in contrast to only one stable fixed point for linear autocatalysis). This means that each of the n competitors can decide the contest in its own favor, depending on initial population numbers. Once the winner is established, there is no easy way for any competitor to grow up and replace it. We therefore

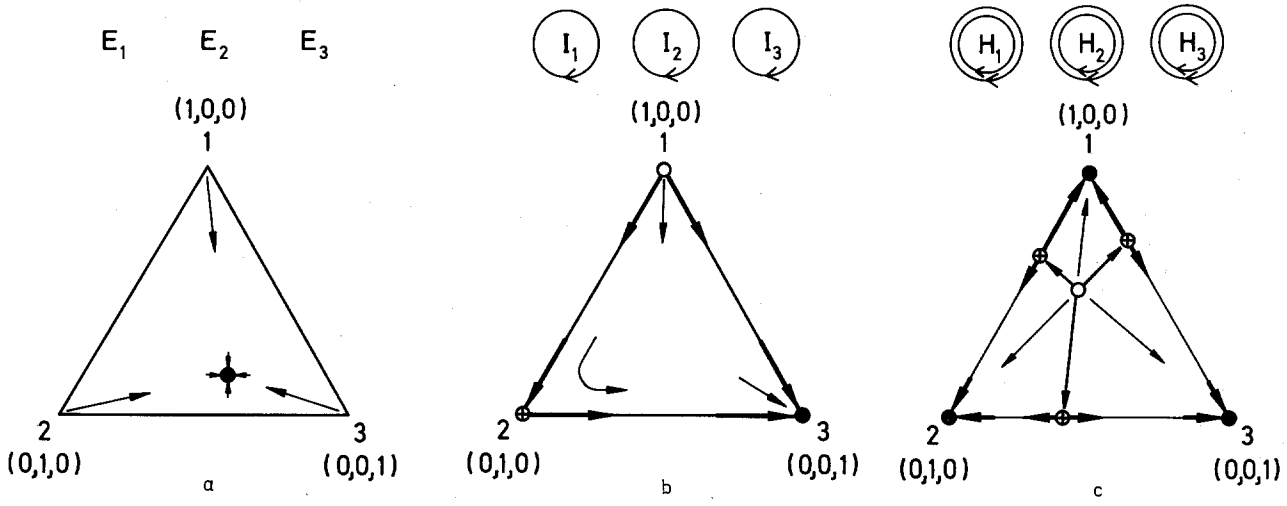

Fig. 22. Three-dimensional fixed-point maps for different types of independent competitors at constant organization. (The symbols E, (I), and (H) have been introduced in Fig. 10).

a) Constant growth rate ($p=0$),

$$\dot{x}_i = k_i - \frac{x_i}{c_0}\sum_{j=1}^{3} k_j$$

$$k_1=1; \quad k_2=2; \quad k_3=3.$$

The map shows a focus inside the unit simplex S_3 which means stable and coexistent behavior of all three species. It is easy to visualize the whole manifold of trajectories approaching the stable focus along straight lines through every point in S_n.

b) Linear growth rate ($p=1$),

$$\dot{x}_i = k_i x_i - \frac{x_i}{c_0}\sum_{j=1}^{3} k_j x_j \qquad k_1=1; \quad k_2=2; \quad k_3=3.$$

A pure state consisting of species 3 represents the only stable long-time-range solution of the system. With the exception of the two edges $\overline{12}$ and $\overline{23}$ all trajectories start in point 1 and end in point 3.

c) Quadratic growth rate ($p=2$),

$$\dot{x}_i = k_i x_i^2 - \frac{x_i}{c_0}\sum_{j=1}^{n} k_j x_j^2 \qquad k_1=1; \quad k_2=2; \quad k_3=3.$$

The simplex S_3 is split into three regions, each being a basin for a stable fixed point. The size of the basin is correlated directly with the values of the corresponding rate constants. Since k_3 is largest the fixed point $\bar{\mathbf{x}}_3$ has the largest basin

call this situation 'once-for-ever selection'. As in the two preceding cases the fixed-point map does not depend on the total concentration c_0.

The two other classes of fixed points include one source in the interior of the unit simplex (all coordinates being finite) and 2^n-n-2 saddle points, one on each edge and one in each face (including all possible hyperfaces) of S_n. Both classes of fixed points represent unstable behavior. We dispense with listing their coordinates and normal modes; they can be obtained by straightforward computations. Instead we illustrate the typical selection behavior of the different growth systems by showing some examples of unit simplices of dimension 3 (cf. Fig. 22).

The three relatively simple model cases have been chosen to exemplify the method of fixed-point analysis and to stress those properties we have to watch out for. The nature of the fixed point, especially whether it provides stable or unstable solutions, is of utmost importance for problems of selection and evolution. Of no less significance is the position of the fixed points in the unit simplex. Cooperative selection of a set of replicative units requires the fixed point to lie in the interior of the unit simplex S_k referring to a subspace $\mathbb{X}^k$ formed by the concentration coordinates of the k cooperating units. On the other hand, the position of a sink at one of the corners of S_k is representative of competition, leading to selection of only one component, while positions at edges, faces, or hyperfaces indicate partial competition and selection.

The build-up of a translation apparatus, for instance, requires the concomitant selection of several replicative units as precursors of different genes. None of the three systems discussed above fulfils the requirements for such a concomitant selection. The first system appears to be coexistent, but it is not selective and therefore cannot evolve to optimal function. The second system allows for coexistence only within narrow limits of the quasi-species distribution; it does not tolerate divergence of the genotypes, which is required to facilitate phenotypic diversification. The third system, finally, is strongly anticooperative, to such an extent that a species, once established, selects against any mutant, whether or not it provides a selective advantage.

Following up the suggestions which emerged from the comparative review in Section V we shall now investigate more closely ensembles with functional linkages. They will have to include replicative units for the purpose of conservation of the genetic information, at the same time they will have to be stabilized cooperatively via couplings, which will cause the growth function to be inherently nonlinear. The properties to be expected for the linked system hence will bear some relation to the third example of independent competitors.

b) Catalytic Chains

The most direct way of establishing a connection among all members of an ensemble is to build up a chain via reactive couplings, much as we link words into sentences in our language (Fig. 23).

The rate terms referring to these couplings will cause the net growth functions Γ_i for all but the first member to be nonhomogeneous:

$$\dot{x}_1 = k_1 x_1 - \frac{x_1}{c_0}\left[k_1 x_1 + \sum_{j=2}^{n}(k_j x_j + k'_j x_j x_{j-1})\right]$$

$$\dot{x}_i = k_i x_i + k'_i x_i x_{i-1} - \frac{x_i}{c_0}\left[k_1 x_1 + \sum_{j=2}^{n}(k_j x_j + k'_j x_j x_{j-1})\right]$$

for $i=2,3,\ldots,n$. (58)

Due to the lack of homogeneity the fixed-point maps will be of a more complicated form than in the cases discussed thus far.

To keep the procedure lucid we start with a three-dimensional system and extend our analysis later to higher dimensions. Table 8 contains a compilation of the pertinent relations of dimension three together with a brief characterization of the fixed-point map. According to this

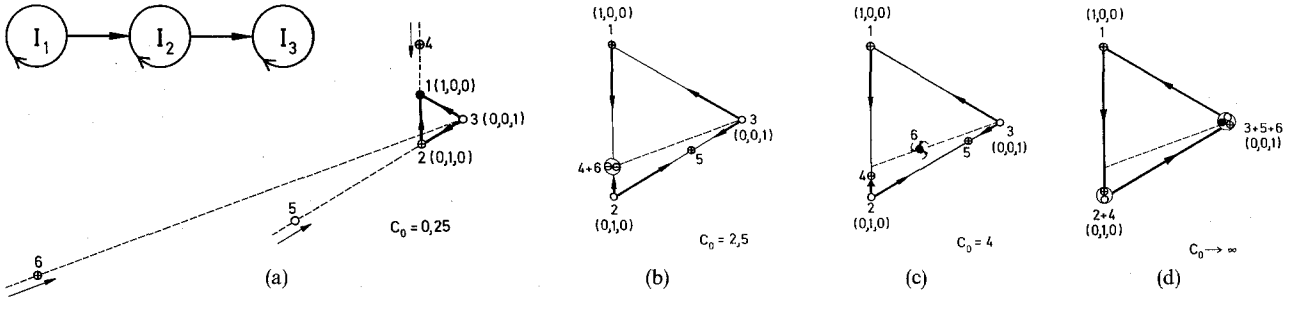

Fig. 23. Fixed-point maps of a catalytic chain of self-replicative units (I_i) under the constraint of constant organization:

$\Gamma_1 = k_1 x_1$;

$\Gamma_i = k_i x_i + k'_i x_i x_{i-1}$ (for $i=2,3$)

$k_1=3$; $k_2=2$; $k_3=1$; $k'_2=2$; $k'_3=1$

$1=\bar{\mathbf{x}}_1$; $2=\bar{\mathbf{x}}_2 \ldots 6=\bar{\mathbf{x}}_6$

At low concentrations (a) the stable solution corresponds to selection of species 1. If the two other species, however, have not yet been extinguished when the total concentration reaches a critical value, a new stationary state emerges, at which all three species become stable (b). With a further increase of the total concentration (c), only species 3 is favored so that the final situation (d) is equivalent to a selection of species 3. The underlying mechanism, however, differs from that for independent competitors

Table 8. Fixed-point analysis of catalytic chains of dimension three

The fixed-point map shows six fixed points with the coordinates and normal modes as given below:

$\bar{\mathbf{x}}_1=\begin{pmatrix}c_0\\0\\0\end{pmatrix}$	$\bar{\mathbf{x}}_2=\begin{pmatrix}0\\c_0\\0\end{pmatrix}$	$\bar{\mathbf{x}}_3=\begin{pmatrix}0\\0\\c_0\end{pmatrix}$
$\omega_1^{(1)}=k_3-k_1$	$\omega_1^{(2)}=k_1-k_2$	$\omega_1^{(3)}=k_1-k_3$
$\omega_2^{(1)}=k_2'c_0-k_1+k_2$	$\omega_2^{(2)}=k_3'c_0-k_2+k_3$	$\omega_2^{(3)}\quad k_2-k_3$
$\bar{\mathbf{x}}_4\begin{pmatrix}\frac{k_1-k_2}{k_2'}\\ \frac{k_2'c_0-k_1+k_2}{k_2'}\\0\end{pmatrix}$	$\bar{\mathbf{x}}_5\begin{pmatrix}0\\ \frac{k_2-k_3}{k_3'}\\ \frac{k_3'c_0-k_2+k_3}{k_3'}\end{pmatrix}$	$\bar{\mathbf{x}}_6\begin{pmatrix}\frac{k_1-k_2}{k_2'}\\ \frac{k_1-k_3}{k_3'}\\ \kappa\end{pmatrix}$
$\omega_1^{(4)}=\frac{(k_2'c_0-k_1+k_2)(k_2-k_1)}{k_2'c_0}$	$\omega_1^{(5)}=k_1-k_2$	$\kappa=\frac{k_2'k_3'c_0-k_3'(k_1-k_2)-k_2'(k_1-k_3)}{k_2'k_3'}$
$\omega_2^{(4)}=\frac{1}{k_2'}\{k_2'k_3'c_0-k_3'(k_1-k_2)-k_2'(k_1-k_3)\}$	$\omega_2^{(5)}=\frac{(k_3'c_0-k_2+k_3)(k_3-k_2)}{k_3'c_0}$	$\omega_1^{(6)}$ and $\omega_2^{(6)}$ are the eigenvalues of the Jacobian matrix $\mathbf{A}(\mathbf{x}=\bar{\mathbf{x}}_6)$.

The three fixed points $\bar{\mathbf{x}}_1$, $\bar{\mathbf{x}}_2$, and $\bar{\mathbf{x}}_3$ coincide with the corners of the unit simplex S_3 (cf. Fig. 23) and hence signify competitive behavior – irrespective of their nature. The positions of the three other fixed points depend (linearly) on the total concentration c_0. The two fixed points $\bar{\mathbf{x}}_4$ and $\bar{\mathbf{x}}_5$ move along the edges $\overline{12}$ and $\overline{23}$ of the simplex, thereby showing partial competition. Solely the fixed point $\bar{\mathbf{x}}_6$ may pass through the interior of S_3 yielding cooperative selection of all chain members.

At low total concentration:

$$c_0<(k_1-k_2)/k_2', \quad (k_2-k_3)/k_3' \quad \text{or} \quad (k_1-k_3)/k_3'$$

the position of the fixed point $\bar{\mathbf{x}}_4$, $\bar{\mathbf{x}}_5$, or $\bar{\mathbf{x}}_6$, respectively, lies outside the simplex S_3, which means outside a physically meaningful region of the concentration space. (At least one concentration coordinate is negative.) For $c_0\to 0$ the positions of these fixed points even approach infinity. The dynamic system becomes asymptotically identical with the system of exponentially growing (noncoupled) competitors, characterized by the fixed points $\bar{\mathbf{x}}_1$, $\bar{\mathbf{x}}_2$, and $\bar{\mathbf{x}}_3$.

If $k_1>k_2$, k_3 and c_0 is above a threshold given by the sum of $[(k_1-k_2)/k_2']+[(k_1-k_3)/k_3']$, the fixed point $\bar{\mathbf{x}}_6$, indicating cooperative behavior, enters the unit simplex. However, it does not approach any point in the interior of S_3, but rather migrates toward the corner **3**.

analysis, the three members (I_1 to I_3) of the linear chain of self-reproductive units can be selected concomitantly only under very special conditions, namely

$$k_1>k_2, k_3 \tag{59}$$

and

$$c_0>\frac{k_1-k_2}{k_2'}+\frac{k_1-k_3}{k_3'} \tag{60}$$

It seems very unlikely that partners which happen to fulfill condition (59) can maintain it over long phases of evolution (which means that mutations that change relation (59) must never occur). Even if they are able to do so, the system will then develop in a highly asymmetric manner, whereby – at least under selection constraints – only the population number of the last member in the chain increases with c_0. Being aware that this soon means a divergence of population numbers by orders of magnitude, we may conclude that such a system will not be able to stabilize a joint function, since it cannot control the relative values of population numbers over a large range of total concentrations.

This behavior is illustrated with some examples in Figure 23, presenting some snapshots of a continuous process in a system growing in a stage close to internal equilibrium. For concentrations c_0 below the critical value given by Equation (60), the three fixed points $\bar{\mathbf{x}}_4$, $\bar{\mathbf{x}}_5$, and $\bar{\mathbf{x}}_6$ lie outside the unit simplex (Fig. 23a). If c_0 equals the critical value, the fixed point $\bar{\mathbf{x}}_6$ reaches the boundary of the simplex (Fig. 23b) and, with increasing c_0, migrates through its interior. At the same time it has changed its nature, now representing a stable fixed point (Fig. 23c), which in this particular case is a spiral sink. (A more detailed presentation of fixed-point analysis with inhomogeneous growth functions will be the subject of a forthcoming paper [53]). Figure 23d indicates the final fate of this stable fixed point, namely, migration to the corner **3**. The system thereby approaches the pure state $\bar{x}_3=c_0$.

The relevant results obtained for three dimensions can be generalized easily for the n-dimensional system. The role of species **3** is now taken by species **n**. Instead of six we find $2n$ fixed points. The most interesting fixed point is $\bar{\mathbf{x}}_{2n}$. Its position can easily be determined:

$$\bar{\mathbf{x}}_{2n}=\begin{pmatrix}\frac{k_1-k_2}{k_2'}\\ \frac{k_1-k_3}{k_3'}\\ \vdots\\ c_0-\sum_{j=2}^{n}\frac{k_1-k_j}{k_j'}\end{pmatrix} \tag{61}$$

If and only if the rate constants fulfil the relations $k_1 > k_j, j=2,3,\ldots,n$ and the total concentration exceeds the critical value:

$$c_{cr} = \sum_{j=2}^{n} \frac{k_1 - k_j}{k'_j} \tag{62}$$

the fixed point $\bar{x}_{2n}$ lies inside the simplex S_n. Then, $\bar{x}_{2n}$ corresponds to a stable stationary state. All concentrations besides $\bar{x}_n$ are constant at this state and hence the system approaches the pure state $\bar{x}_n = c_0$ at large total concentrations.

We may summarize the behavior of catalytic chains:
1) Stable sationary states exist only when the rate constants and the total concentration fulfil certain relations:

$$k_1 > k_j; \quad j=2,3,\ldots,n; \quad c_0 > \sum_{j=2}^{n} \frac{k_1 - k_j}{k'_j}$$

The system must be subject to selection constraints in order to select against other nonfunctional units, and the required order of rate constants must not be changed by selection of favorable mutants.
2) Provided the conditions given in (1) are fulfilled, the concentrations of individual species are of a comparable magnitude only in a rather small range of total concentrations. With increasing values of c_0 the last member of the chain, I_n, grows under (quasi-)stationary conditions and finally will dominate exclusively.
The catalytic chain therefore is not likely to be useful as an information-integrating system.

c) Branched systems

Wherever coupled systems evolve, branching of couplings as depicted in Figure 24 will be inevitable. Fixed-point analysis of such branched networks does not reveal any unexpected, new features. At very low total concentrations the three species behave like independent competitors. There are now two critical values of c_0, at which either I_1 and I_2 or I_1 and I_3 become coexistent. This finally depends on whether I_2 or I_3 is more efficiently favored by I_1. One of the two fixed points turns out to be a stable node, the other a saddle point. At higher total concentration the stable fixed point again migrates toward one of the corners 2 or 3, respectively. An illustration of this behavior is given in Figure 24.

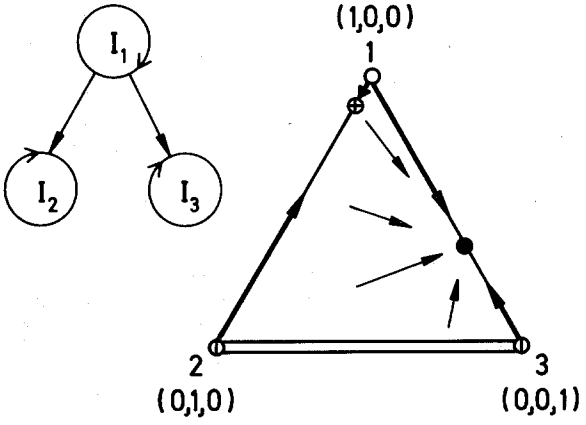

Fig. 24. Fixed-point map of a dynamic system representing a branching point in a catalytic network of self-replicative units (I_i) under the constraints of constant organization

$\Gamma_1 = k_1 x_1; \quad \Gamma_i = k_i x_i + k'_i x_i x_1$ (for $i=2,3$)

$k_1 = 3; \quad k_2 = k_3 = 0; \quad k'_2 = 1; \quad k'_3 = 2; \quad c_0 = 3.5$

The three-dimensional system investigated here can be generalized in two ways:
1. More than two branches may start out from a given point.
2. The individual branches may contain more than one member. The results of fixed-point analysis of these many-dimensional systems are essentially the same as those obtained in three dimensions and can be summarized as follows:

Branched systems of self-replicative units are not stable over long time spans. The branch which is most efficient in growing will be selected while other branches will disappear. What remains finally is the most efficient linear chain and thereby the whole problem is reduced to a dynamic system of type (58), which we have discussed in the previous section.

VII.7. Fixed-Point Analysis of Hypercycles

a) Classification

Ring closure in dynamic systems leads to entirely new properties of the system as a whole, as we have seen in Part A. The set of molecules which are formed in a closed loop of chemical reactions represents a catalyst. A cycle of catalysts (Fig. 4) in turn has autocatalytic properties and may be regarded as a self-replicative system. After finding that straightforward or branching couplings among self-replicative units do not lead to a joint selection of the functionally linked system, we may ask whether any ring closure in the chain of couplings will bring about a change in the nature of the selective behavior of the total ensemble. We might argue that this must be the case, since we remember that in open chains the recipient of all the benefits of coupling was always the last member.
Hypercycles have been generally classified in Part A. The simplest constituents of this class of networks are obtained by a straightforward functional link among self-replicative units as shown in Figure 25.
This section on hypercycles will consist of three different parts. First we present some definitions and useful criteria for classification of this new kind of catalytic system. Then the results of fixed-point analysis for the most important 'pure' types of hypercycles are described. Finally, we shall study one example of a self-organizing system which represents a realistic catalytic hypercycle.

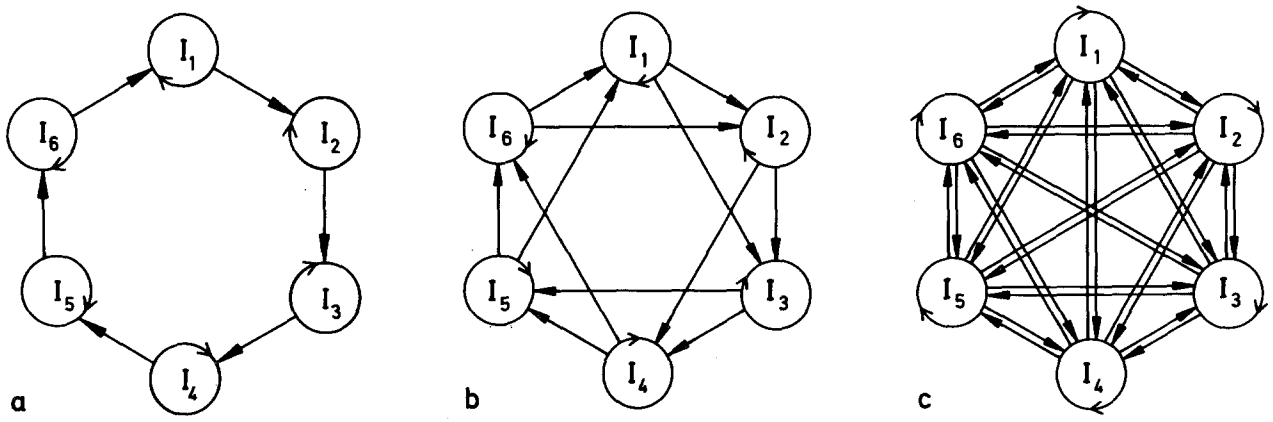

Fig. 25. Catalytic hypercycles, a) degree $p=2$, $n=6$, b) degree $p=3$, $n=6$, and c) degree $p=n=6$

Primarily, hypercycles differ from ordinary catalytic cycles by nonlinear terms in the growth rates. In simple cases, the functions Γ_i will be products of concentrations as shown in Equation (63). The exponents $p_{\lambda i}$ according to

$$\Gamma_i = k_i \prod_{\lambda=1}^{n} x^{p_{\lambda i}} \tag{63}$$

can be regarded as elements of a matrix **P**. The indices λ and i denote which population variable (x_λ) has to be raised to the power $p_{\lambda i}$ in the function Γ_i. The dynamic system is then determined completely by the matrix of exponents **P**, by the vector of rate constants $\mathbf{k}=(k_1 \ldots k_n)$, and by a set of initial conditions. At first we shall study the 'pure' cases only, which are characterized by homogeneous growth terms Γ_i. The requirement of homogeneity leads to a first restriction for the exponents in the matrix **P**:

$$\sum_{\lambda=1}^{n} p_{\lambda i} = p; \quad i=1,2,\ldots,n \tag{64}$$

'p' is now common for all n differential equations and represents the degree of the growth functions introduced in Section V. In addition to the restriction of homogeneity we shall allow individual concentrations to appear only as first-order terms in Γ_i. Some important cases with higher-order dependences will be discussed below. Accordingly, the exponents $p_{\lambda i}$ are restricted to just two possible values: $p_{\lambda i}=\{0,1\}$.
Finally, we shall introduce cyclic symmetry into the net growth function:

$$\begin{aligned}
&\Gamma_i = k_i x_i x_j x_k x_l \ldots x_r \\
&j=i-1+n(\delta_{i1}); \quad l=i-3+n(\delta_{i1}+\delta_{i2}+\delta_{i3}); \ldots \\
&k=i-2+n(\delta_{i1}+\delta_{i2}); \quad r=i-p+n\sum_{\mu=1}^{p-1}\delta_{i\mu}
\end{aligned} \tag{65}$$

The assumption of cyclic symmetry is not essential for the most important features of the solutions. It is a reasonable assumption, however, if no further information on structural differences in the kinetic equations for the individual members of the cyclic system is available. The matrix **P** is of general and simple form now. A concrete example, the matrix **P** with $n=6$ and $p=3$ is shown below:

$$\mathbf{P}(n=6,p=3)=\begin{pmatrix} 1&0&0&0&1&1 \\ 1&1&0&0&0&1 \\ 1&1&1&0&0&0 \\ 0&1&1&1&0&0 \\ 0&0&1&1&1&0 \\ 0&0&0&1&1&1 \end{pmatrix} \tag{66}$$

Hypercycles with cyclic symmetry and homogeneous growth functions Γ_i thus are completely determined by the values of n and p and the vector **k**.

Schematic diagrams for three examples of hypercycles with $n=6$ and $p=2,3$ and n are shown in Figure 25. Cases with $p=1$ must be excluded from the general class of catalytic systems called hypercycles, since they fall into the family of systems with linear growth rates Γ_i.

b) General Analysis

A summary of fixed-point analysis of hypercyclic systems is given in Table 9.
We discuss two cases which are most important in the context of this paper.
1. The simplest hypercycle possible with $p=2$
2. The hypercycle, which utilizes catalytic links among all members, i.e., $p_{\lambda i}=1$ for $i=1,\ldots,n$ and $\lambda=1,\ldots,n$, and hence, $p=n$
The first system we christen simply 'elementary hypercycle', the second – in accordance with its most common physical realization as a cooperatively behaving complex – 'compound hypercycle'.

c) The Elementary Hypercycle

Depending on the dimension of the dynamic system, we observe interesting changes in the nature of the fixed point in the center of the simplex. For this purpose we inspect more closely the sets of eigenvalues obtained for different values of n, which are described appropriately as vectors, $\omega = \mathrm{Re}\,\omega\,\mathbf{e}_1 + i\,\mathrm{Im}\,\omega\,\mathbf{e}_2$ in the complex Gaussian plane (Fig. 26). The fixed point in the center is a focus for $n=2$, a spiral sink for $n=3$, a center for $n=4$. For $n\geqq 5$ we obtain saddle points with spiral components in some planes. These characteristic changes in the nature of a fixed point are reminiscent of a Hopf bifurcation despite the fact that our parameter is a

Table 9. The fixed-point map of a hypercycle

Subjecting the dynamic system (65) to the condition of constant organization we find:

$$\dot{x}_i = k_i x_i x_j \dots x_l - \frac{x_i}{c_0} \sum_{r=1}^{n} k_r x_r x_s \dots x_t$$

$$j = i-1+n\delta_{i1}, \dots, l = i-p+1+n\sum_{\mu=1}^{p-1}\delta_{i\mu}$$

$$s = r-1+n\delta_{r1}, \dots, t = r-p+1+n\sum_{\mu=1}^{p-1}\delta_{r\mu};\ p \leqq n \qquad \text{(T.9.1)}$$

Fixed-point analysis can be carried out *analytically* for any value of n if all the rate constants[a] are equal:

$$k_1 = k_2 = \dots = k_n = k \qquad \text{(T.9.2)}$$

The results obtained are:
1) One fixed point, which we denote by $\bar{\mathbf{x}}_0$, is always positioned in the center of the concentration simplex.
2) n additional fixed points occur at the corners of the simplex S_n: $\bar{\mathbf{x}}_1, \bar{\mathbf{x}}_2, \dots, \bar{\mathbf{x}}_n$.

[a] Variations in the individual rate constants on the solutions will be discussed in Section VIII.

3) In many cases there are also one-, two-, three-, or even higher-dimensional manifolds of fixed points, e.g., fixed-point edges, triangles, tetrahedra, and higher-dimensional simplices [54]. These manifolds always occur in the boundaries of the corresponding simplices S_n, for example, fixed-point edges are found in the boundaries of S_n, $n \geqq 4$, fixed-point triangles in the boundaries of S_n, $n \geqq 6$, and fixed-point tetrahedra on S_n, $n \geqq 8$.
Normal-mode analysis around the central fixed point $\bar{\mathbf{x}}_0$, which is responsible for cooperative selection, yields:

$$\bar{\mathbf{x}}_0 = \begin{pmatrix} 1 \\ 1 \\ \vdots \\ 1 \end{pmatrix} \cdot \frac{c_0}{n}; \qquad \omega_j^{(0)} = -\frac{1-\gamma^{-(p-1)}}{1-\gamma}\left(\frac{c_0}{n}\right)^{p-1} \cdot k$$

$$j = 1, 2, \dots, n-1; \qquad \gamma = e^{\frac{2\pi i}{n} j}$$

$$\omega_n^{(0)} \equiv \omega_c^{(0)} = -\left(\frac{c_0}{n}\right)^{p-1} \cdot k \qquad \text{(T.9.3)}$$

For $p=2$ there are n or $n-1$ distinct eigenvalues, while for $p=n$ all eigenvalues are equal to $\omega_c^{(0)}$. The first case is the usual situation. $n-1$ single and one double-degenerate eigenvalues $\omega_c^{(0)} = \omega_{j=n/2}^{(0)} = -k(c_0/n)^{p-1}$ are obtained for $p=2$ and even n, whereas for odd n all the eigenvalues are distinct. The negative value of $\omega_c^{(0)}$ again indicates that the dynamic system on the simplex S_n is stable against fluctuations in total concentration c.

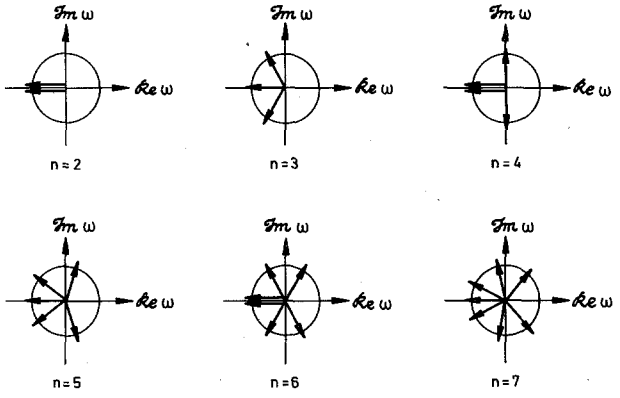

Fig. 26. Normal modes ω for the central fixed point ($\bar{\mathbf{x}}_0$) in hypercycles of type (65) with $p=2$ and dimension n. Reω and Imω stand for imaginary and real part of the frequency ω, respectively

discretely varying quantity, the dimension n of the dynamic system. As we shall show by a more general analysis in Section VIII the central fixed point is asymptotically stable for $n=2, 3,$ *and* 4. In the case of higher dimensions $n \geqq 5$ we find a more complex attractor, namely, a stable closed orbit or limit cycle, which always remains inside the simplex and therefore never reaches the boundary. In the latter case, time averages of concentrations x_i:

$$X_i(t) = \frac{1}{t}\int_0^t x_i(\tau)\,\mathrm{d}\tau, \qquad \bar{X}_i = \lim_{t\to\infty} x_i(t) \qquad (67)$$

rapidly approach c_0/n (for equal k_i values), which is just the same value as in the case of stable fixed points.
For the fixed point at any corner k ($x_k = c_0$) of S_n we find one positive and $n-1$ zero $\omega_j^{(k)}$ values. In Section VIII we shall analyze the nonlinear contributions and identify these fixed points as saddle points. The corresponding long-term solutions hence do not contribute to the selection behavior.
The fixed-point map for a hypercycle with $p=2$ and $n=3$ is shown in Figure 27 for a concrete example.

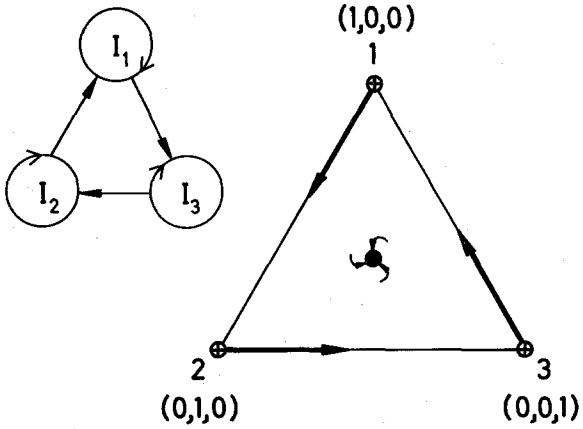

Fig. 27. Fixed-point map of a dynamic system (65) consisting of self-replicative units (I_i) forming a hypercycle under the constraint of constant organization

($\Gamma_i = k_i x_i x_j$; $j = i-1+n\delta_{i1}$; $n=3$, $p=2$, $\mathbf{k}=(1, 1, 1)$)

In general, the net growth functions for the individual self-replicative units which form the dynamic system of a hypercycle will contain not only catalytic terms but also first-order growth terms:

$$\Gamma_i = k_i x_i + k'_i x_i x_j \tag{68}$$

Subjecting a dynamic system with these growth functions to the constraints of constant organization we obtain:

$$\dot{x}_i = k_i x_i + k'_i x_i x_j - \frac{x_i}{c_0} \sum_k (k_k x_k + k'_k x_k x_l) \tag{69}$$

$$j = i - 1 + n\delta_{i1}, \quad l = k - 1 + n\delta_{k1}; \quad i = 1, 2, \ldots, n$$

From a mathematical point of view the catalytic chain (Fig. 23) differs from the hypercycle just by a single rate constant and results from the latter by putting $k'_1 = 0$. We may therefore expect some similarities between the two types of dynamic systems. Consistent with the inhomogeneity of the growth functions, the fixed-point maps depend on the total concentration. At the low concentration limit both systems become identical with the system of exponentially growing, indepedent competitors (Fig. 22). At high concentrations, on the other hand, the two systems will differ. The dynamic system (69) asymptotically resembles that of the corresponding elementary hypercycle ($p = 2$).

As a concrete example we consider again a system of dimension $n = 3$. There are seven fixed points: Three coincide with the corners of the simplex S_3, three other fixed points lie on the edges, and the seventh is in the interior of S_3.

Numerical results were calculated for a given set of parameters **k** and are shown in Figure 28. As for the catalytic chain in Figure 23 we present fixed-point maps for three different values of total concentration c_0, which represent low and high concentration limits (**a** and **c**) as well as the critical point

(**b**, $c_0 = c_{or} = k_3(k'^{-1}_1 + k'^{-1}_2) - k_1 k'^{-1}_1 - k_2 k'^{-1}_2$).

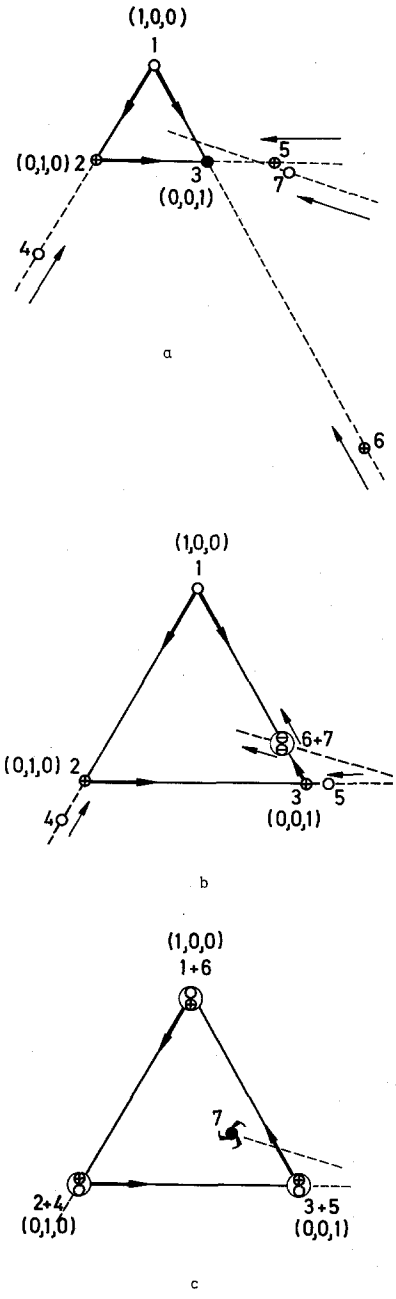

Fig. 28. Fixed-point map of a dynamic system (69) consisting of self-replicative units forming a catalytic hypercycle

($\Gamma_i = k_i x_i + k'_i x_i x_j$, $j = i - 1 + n\delta_{i1}$;
$n = 3$, $p = 2$, $\mathbf{k} = (1, 2, 3; 1, 2, 3)$;
a) $c_0 = 0.5$, b) $c_0 = 2.5$, c) $\lim c_0 \to \infty$;
$\mathbf{1} = \bar{\mathbf{x}}_1$, $\mathbf{2} = \bar{\mathbf{x}}_2$, $\mathbf{3} = \bar{\mathbf{x}}_3$, $\mathbf{4} = \bar{\mathbf{x}}_{12}$, $\mathbf{5} = \bar{\mathbf{x}}_{23}$, $\mathbf{6} = \bar{\mathbf{x}}_{31}$, and $\mathbf{7} = \bar{\mathbf{x}}_0$)

Considering the development of the dynamic systems (58) and (69) close to internal equilibrium, we realize a very important difference between the cyclic and noncyclic systems: The cyclic system leads to an asymptotic high concentration limit which is characterized by constant relative concentrations of the individual species, whereas the open chain approaches the pure state ($x_n = c_0$) at high total concentration.

Summing up the whole development from low to high concentration limits we realize that a hypercycle, as described by the dynamic system (69), is an appropriate example of self-organization. Starting from competition among individual species the growing system approaches a final state with dynamically controlled net production of all members. This internal control leads to a stable stationary state or to a state with regular oscillation of population variables about a fixed point.

d) The Compound Hypercycle

The analysis of the case $p = n$ leads to a simple, general result: As in the other example treated before, there is one fixed point inside the simplex. The whole boundary of the simplex, however, consists of unstable fixed points, fixed-point edges, fixed-point planes, etc. Since the invariant point in the middle ($\bar{\mathbf{x}}_0$) is a focus for all values of n, all trajectories starting from the interior of the simplex, which is the whole physically meaningful domain, will approach this particular point after long enough time. All the eigenvalues $\omega_j^{(0)}$ associated with $\bar{\mathbf{x}}_0$

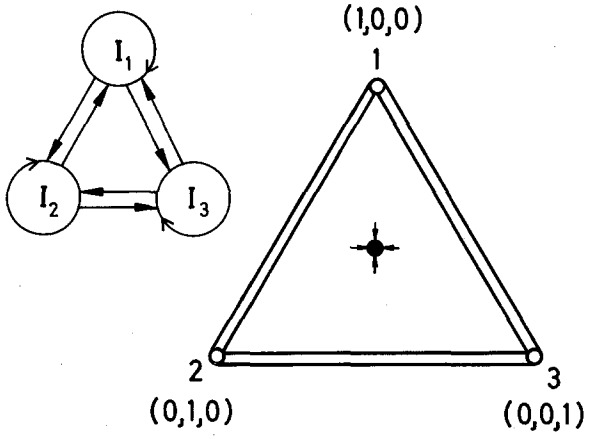

Fig. 29. Fixed-point map of a dynamic system (65) consisting of self-replicative units (I_i) forming a compound hypercycle under the constraint of constant organization

($I_i = k_i x_1 x_2 \ldots x_n$; $n=3$, $p=3$, $\mathbf{k}=(1, 1, 1)$)

are the same for given values of k, c_0, and n. They follow from the expression (3) given in Table 9 if we set $p=n$. The fixed-point map for a compound hypercycle with $n=3$ is shown in Figure 29. The complexes, thus, represent excellent examples for the control of relative concentrations of their constituents.

e) Comparison of Various Hypercycles

Hypercycles have an intrinsic capability for integrating information. Indeed the simplest members of this class represent the least complicated dynamic structures that are able to prevent an ensemble of functionally linked self-replicative units from destroying information by elimination of some of their members as a result of selective competition. From the dynamic point of view, all kinds of hypercycles are equivalent with respect to this property. On the other hand, less sophisticated systems, such as simple catalytic cycles (Fig. 4), are not eligible as information-integrating systems since they lack the property of *inherent* self-reproducibility (cf. [4], p. 501ff.).

A further discrimination within the hierarchy of hypercycles can be made according to their realizability in nature, which will be the subject of Part C. To present one example of such an argument, we compare here the simple type of hypercycle ($p=2$) and the complex ($p=n$) with respect to their physical materialization. Simple hypercycles require bimolecular encounters of macromolecules according to their growth law. These bimolecular terms can easily be provided by various mechanisms and also result from realistic assumptions about nucleic acid replication or messenger-instructed protein synthesis (see also Section IX and Part C). A compound hypercycle requires all partners to contribute to the rate of formation of each constituent. A mechanism leading to such a compound hypercycle then would need either a – highly improbable – multimolecular encounter or an intermediate formation of a complex of n different subunits, which is highly disfavored at low concentrations. Prebiotic conditions, on the other hand, are characterized by exceedingly low concentrations of *individual* macromolecules. For an efficient start of evolution via compound hypercycles one would have to assume extremely high association constants far outside the range of experimental experience and an inherent linkage between these constants and the functional efficiency of the single constituents. The compound hypercycle is thus likely to be of less importance for the nucleation of a translation system than any hypercycle of lower degree p. In more advanced phases of precellular evolution compound hypercycles might have had a chance to form.

Various systems consisting of catalytically active and self-reproductive units have been studied by fixed-point analysis. The results provide clear evidence for the necessity of hypercyclic coupling. Only catalytic hypercycles can fulfill the criteria for integration of information listed in Section IV.5.

1. Selective stability of each component due to favorable competition with error copies

2. Cooperative behavior of the components integrated into the new functional unit

3. Favorable competition of the functional unit with other less efficient systems

VIII. Dynamics of the Elementary Hypercycle

Hypercycles, being the relevant systems of prebiotic self-organization, deserve a more detailed analysis of their dynamic behavior. A complete qualitative description can be given for the class of elementary hypercycles ($p=2$) up to dimension $n=4$. For higher dimensions, as well as for hypercycles of a more complex structure, we have to aid the topologic analysis by numerical integration. We exemplify the methods with the class of elementary hypercycles, which reveal all the basic properties of hypercyclic self-organization.[1]

VIII.1. Qualitative Analysis

Since we are concerned with dynamic systems of cooperating constituents, the stable attractors in the interior of the physically accessible range of concentrations are of primary interest. More

[1] For a particular case of a hypercycle, in which the second-order term $x_k x_{k-1}$ of the growth function has been substituted by a term of the form $x_k \ln x_{k-1}$, an analytical solution could be provided [21].

specifically, we have to study the stability of those fixed points, for which some eigenvalues of the Jacobian matrix have zero real parts. In Section VII (Table 9) we encountered essentially two cases:

1. Zero eigenvalues ($\omega_j^{(i)}=0$, $j=2,3,\ldots,n$ and $i=1,2,\ldots,n$) for fixed points $\bar{\mathbf{x}}_i$ at the corners of the simplices S_n
2. Purely imaginary eigenvalues ($\omega_{2,4}^{(0)}=\pm i$) for the central fixed point of the four-membered hypercycle on S_4[2].

Before presenting a general proof for the stability of the central fixed points in hypercycles of low dimensions $n\leqq 4$, let us inspect the topology of these systems in more detail.

The dynamic systems corresponding to elementary hypercycles can be decomposed into several subsystems each of which is defined on a globally invariant subspace. A set of points or a subspace will be called 'globally invariant' with respect to a given dynamic system if and only if a trajectory that passes through any point of the subspace never leaves the subspace.

In particular we find that the dynamic systems on the simplices S_n can be subdivided into those on boundaries (BS_n) and those in the interiors (IS_n). The interior of a simplex, defined as before, is the region where no population variable vanishes: $0<\xi_i<1$, $i=1,2,\ldots,n$. Clearly, the dynamic systems on IS_n are most interesting since they describe the development of intact hypercycles. We denote them in the following by numbers: **2**, **3**, **4**, ... **N**.

On the boundary, one, two, or more population variables vanish. Consequently, the dynamic systems on BS_n can be subdivided into dynamic systems on simplices of lower dimension like edges, faces, and hyperfaces. To distinguish these systems from complete hypercycles we shall use **2A**, **2B**, **3A**, etc. as short-hand notations. All dynamic systems corresponding to elementary cycles of dimension $n\leqq 4$ are shown schematically in Figure 30. As a concrete example, the decomposition of the four-dimensional system into 11 subsystems is presented in Table 10.

Table 10. Globally invariant dynamic subsystems of the elementary hypercycle with dimension $n=4$

Symbol	Condition	Dynamic system
4	$\xi_1,\xi_2,\xi_3,\xi_4>0$	$\dot{\xi}_i=\xi_i\xi_j-\xi_i\phi$, $i=1,2,3,4$ $j=i-1+n\delta_{i1}$ and $\phi=\xi_1\xi_2+\xi_2\xi_3+\xi_3\xi_4+\xi_4\xi_1$
3A	$\xi_4=0$	$\dot{\xi}_1=-\xi_1\phi$ $\dot{\xi}_i=\xi_i\xi_j-\xi_i\phi$, $i=2,3$ $j=i-1$ and $\phi=\xi_1\xi_2+\xi_2\xi_3$
	$\xi_3=0$, $\xi_2=0$ or $\xi_1=0$	analogously
2A	$\xi_3=\xi_4=0$	$\dot{\xi}_1=-\xi_1\phi$, $\phi=\xi_1\xi_2$ $\dot{\xi}_2=\xi_1\xi_2-\xi_2\phi$
	$\xi_2=\xi_3=0$, $\xi_1=\xi_2=0$ or $\xi_4=\xi_1=0$	analogously
2B	$\xi_2=\xi_4=0$ $\xi_1=\xi_3=0$	$\dot{\xi}_i=0$, $i=1,2,3,4$

All the dynamic systems up to dimension $n=4$ can be analyzed by Lyapunov's method (Table 11). For the three systems **2**, **3**, and **4**, Lyapunov functions are given, and hence, the central fixed point represents a stable attractor. Moreover, the basin of this fixed point extends over the whole interior of the simplices. In more physical terms this means: Starting from any distribution of population variables we end up with the same stable set of stationary concentrations. The dynamic systems indeed are characterized by cooperative behavior of the constituents. This result is of particular importance for the four-dimensional system where the linear approximation, used in fixed-point analysis, yielded a center surrounded by a manifold of concentric closed orbits in the x, y-plane (see Fig. 31a), which does not allow definite conclusions about stability.

[2] Purely imaginary eigenvalues will occur also in elementary hypercycles of dimension $4k$, where k is an integer $\geqq 2$. In these higher-dimensional examples, however, the central fixed point is a saddle point independently of the nature of higher-order contributions to the purely imaginary eigenvalues.

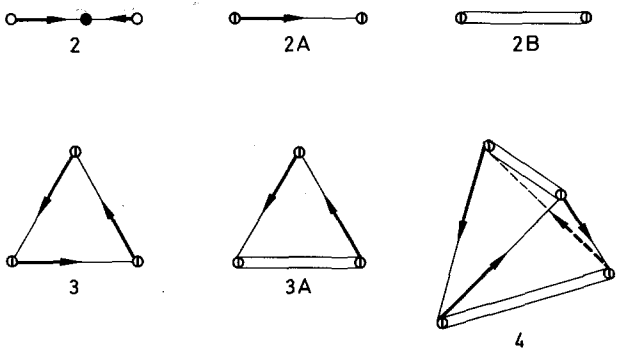

Fig. 30. Dynamic systems corresponding to elementary hypercycles of dimensions $n=2$, 3, and 4. The individual systems are mapped on the simplices S_n and can be decomposed into globally invariant dynamic subsystems (Table 10): The 'complete' subsystem **2**, **3**, and **4** are characterized by nonzero values of all population variables and thus describe the development in the interiors of the simplices $S_n(IS_n$: $0>x_i>c_0$, $i=1,2,\ldots,n)$. On the boundaries of the simplices $S_n(BS_n)$ one or more population variables vanish and dynamic subsystems of lower dimension like the 'flowing edge' **2A**, the 'fixed-point edge' **2B**, and the triangle of type **3A** are obtained (note that the dynamic system **2A** occurs in the boundaries surrounding **3**, **3A**, and **4**, **2B** in those surrounding **3A** and **4**, and **3A** finally occurs in the boundary around **4**)

The dynamic systems on the boundaries of the simplices (BS_n) determine the behavior of 'broken' hypercycles, i.e., catalytic hypercycles which are lacking at least one of their members. In reality, these systems describe the kinetics of hypercycle extinction. They are also of some importance in phases of hypercycle formation. On the boundaries of the complete dynamic systems up to dimension 4 we find two kinds of edges **2A** and **2B** as well as the face **3A** (Fig. 30). All three dynamic systems can be analyzed in a straightforward way.

The first kind of edge **2A** connects two consecutive pure states or corners, which we denote by 'i' and 'j' ($j=i+1-n\delta_{in}$). As shown in Figure 32 there is a steady driving force along the edge, always pointing in the direction $i\rightarrow j$. The only trajectory of this system thus leads from corner i to corner j. Accordingly, we shall call system **2A** a flowing edge. In approaching corner j, the driving force decreases parabolically (Fig. 32). Hence, the linear term of the Taylor expansion vanishes at the fixed point $\bar{\mathbf{x}}_j$, and fixed-point analysis cannot yield the desired prediction as to the nature of this fixed point.

In elementary hypercycles the corners of the simplices are saddle points: A corner (i) is stable with respect to fluctuations along the edge $\overline{hi}$ ($\delta x_h>0$, $h=i-1+n\delta_{i1}$) but unstable along the edge $\overline{ij}$ ($j=i+1-n\delta_{in}$). On the boundary of every complete dynamic system we thus find a closed loop, $\overline{12}\ \overline{23}\ \overline{34}\ldots\overline{n1}$, along which the system has a defined sense of rotation. This cycle is not a single trajectory. A particular kind of fluctuation is required at every corner to allow the system to proceed to the next pure state. The existence of this loop is equivalent to the cyclic symmetry of the total system. The asymmetry at each single corner reflects the irreversibility of biopolymer synthesis and degradation, assumed in our model.

The physically accessible range of variables in the dynamic system **3A** is circumscribed by two consecutive flowing edges, $\overline{ij}$ and $\overline{jk}$ ($j=i+1$

Table 11. Lyapunov functions [57] for basic hypercycles of dimension $n=2, 3$, and 4

To prove the stability of a certain fixed point $\bar{\mathbf{x}}$ of a dynamic system $\dot{\mathbf{x}}=A(\mathbf{x})$, we must find an arbitrary function $V(\mathbf{x})$ which fulfils the following two criteria:

$$(1)\quad V(\bar{\mathbf{x}})=0 \quad \text{and} \quad V(\mathbf{x})>0,\ \mathbf{x}\in U, \tag{T.11.1}$$

i.e., the function vanishes at the fixed point and is positive in its neighborhood U. Thus $V(\mathbf{x})$ has a local minimum at the fixed point.

$$(2)\quad \dot{V}(\mathbf{x})\equiv\frac{\mathrm{d}V}{\mathrm{d}t}=\sum_{j=1}^{n}\left(\frac{\partial V}{\partial x_j}\right)\frac{\mathrm{d}x_j}{\mathrm{d}t}<0, \qquad \mathbf{x}\in U \tag{T.11.2}$$

i.e., the time derivative of $V(\mathbf{x})$ is negative in the neighborhood of the fixed point. For trivial reasons $\dot{V}$ vanishes at $\bar{\mathbf{x}}$: $\dot{V}(\bar{\mathbf{x}})=0$. If it is possible to find such a function $V(\mathbf{x})$ for a given fixed point of a dynamic system, it is called a (strict) Lyapunov function and the point $\bar{\mathbf{x}}$ is (asymptotically) stable: All trajectories passing through a point in the neighborhood of $\bar{\mathbf{x}}$ will end in the fixed point $\bar{\mathbf{x}}$.
A Lyapunov function $V(\mathbf{x})$ may also be defined in a less strict way so as to fulfil the weaker criterion:

$$\dot{V}(\mathbf{x})\leqq 0 \tag{T.11.3}$$

Any trajectory entering the neighborhood U of $\bar{\mathbf{x}}$ will remain there. To give a concrete example; sinks are asymptotically stable in the stronger sense of Lyapunov, whereas centers are stable only with respect to the weaker criterion (T.11.3).
For the sake of convenience we use normalized variables ξ_1 and assume the rate constants to be equal to 1, $k_1=k_2=\cdots=k_n=1$, when we apply Lyapunov's method to basic hypercycles.
The function

$$V=\left(\frac{1}{n}\right)^n-\xi_1\xi_2\ldots\xi_n \tag{T.11.4}$$

has a minimum and vanishes at the fixed point $\xi_i=\frac{1}{n}$ and thus meets condition (T.11.1). The time derivative of V can be obtained by straightforward differentiation

$$\dot{V}=-\xi_1\xi_2\ldots\xi_n(1-nr);$$
$$r=\sum_{k=1}^{n}\xi_k\xi_l; \qquad l=k-1+n\delta_{k1} \tag{T.11.5}$$

Now we have to check criterion (T.11.2) for systems with different values of n. In the interior of the simplex S_n the condition $\dot{V}<0$ becomes equivalent to the inequality

$$r(\xi)<\frac{1}{n}. \tag{T.11.6}$$

Clearly, we find $r(\bar{\xi}_0)=\frac{1}{n}$, which satisfies the equation $\dot{V}(\bar{\xi}_0)=0$. ($\bar{\xi}_0$ represents the central fixed point of the hypercycle.)
For the two-dimensional system ($n=2$), condition (T.11.6) can be easily verified:

$$\xi_1=\xi; \qquad \xi_2=1-\xi\rightarrow r=2\xi(1-\xi)\leqq\tfrac{1}{2} \tag{T.11.7}$$

The function r represents a parabola with the maximum at $\xi=\frac{1}{2}$. Thus $r(\xi)<\frac{1}{2}$ is fulfilled everywhere except at the fixed point $\xi=\frac{1}{2}$, where $r=\frac{1}{2}$. In this case V is a strict Lyapunov function and $\bar{\xi}_0$ is asymptotically stable.
For $n=3$ the situation is very similar. The inequality (T.11.3), $r<\frac{1}{3}$ is valid at every point in the interior of the simplex S_3, except at the fixed point $\bar{\xi}_0$ where $r=\frac{1}{3}$. V again represents a strict Lyapunov function and the central fixed point $\bar{\xi}_0$ is asymptotically stable.
In four dimensions the problem is more involved. We realize that condition (T.11.3) is verified almost everywhere on the simplex S_4:

$$r=(\xi_1+\xi_3)(\xi_2+\xi_4)=s(1-s), \qquad 0\leqq s\leqq 1 \tag{T.11.8}$$

In its interior we find $0\leqq r\leqq\frac{1}{4}$ with $r=\frac{1}{4}$ if and only if $s=\frac{1}{2}$. The equation $s=\frac{1}{2}$ determines the plane $\xi_1+\xi_3=\frac{1}{2}$ (see Figs. 31a and 34b). V apparently is a Lyapunov function solely in the weaker sense. This result suggests that the central fixed point at least is stable. To prove asymptotic stability we introduce new variables x, y, z

$$x=-2(\xi_2+\xi_3)+1 \qquad \dot{x}=-(1+z)(y-xz)$$
$$y=2(\xi_1+\xi_2)-1 \qquad \dot{y}=(1-z)(x-yz)$$
$$z=2(\xi_1+\xi_3)-1 \qquad \dot{z}=z^3-z+x^2-y^2$$

which shift the origin of the coordinate system into the center of the simplex S_4 and place the coordinate axes through the midpoints of the edges $\overline{23}$, $\overline{34}$, and $\overline{13}$, respectively, (cf. Fig. 31a). The fourth variable $\xi_4=1-\xi_1-\xi_2-\xi_3$ is eliminated. The z-axis thus points perpendicular to the critical plane $\xi_1+\xi_3=\frac{1}{2}$, which is spanned by the two variables x and y. In this plane the dynamic system simplifies to $\dot{x}=-y$, $\dot{y}=x$, and $\dot{z}=x^2-y^2$.
The time derivative of z vanishes only along the two lines $x=\pm y$ or $\xi_2=\xi_4$ and $\xi_1=\xi_3$, respectively. Consequently, there is no trajectory in this critical plane – except the fixed point $\bar{\xi}_0$ – and the system will pass through it in infinitely short time. Along any given orbit the condition $\dot{V}(\xi(t))<0$ is fulfilled at almost every moment, the only exceptions being the instances when the critical plane $\xi_1+\xi_3=\frac{1}{2}$ is passed. Along all trajectories, $V(\xi(t))$ is monotonically decreasing with t. V is a strict Lyapunov function, and thus the fixed point $\bar{\xi}_0$ is asymptotically stable.
In higher dimensions $n\geqq 5$, $V(\xi)$ is not a Lyapunov function and therefore no predictions on the stability of the central fixed point can be made by this method.

$-n\delta_{in}$ and $k=j+1-n\delta_{in}$) and one fixed-point edge $\overline{ik}$ ($k\neq i-1+n\delta_{in}$). The trajectories of this system are shown in Figure 31b. They start from some point of the fixed-point edge and end at the corner k, which thus represents the only stable attractor of the system. The species I_k consequently represents the survivor or remnant of this fragment of a hypercycle.
The investigation on the boundaries of basic hypercycles can be generalized to higher-dimensional systems. From the results obtained we can make the desired predictions about the long-term development of broken hypercycles. After one species in a hypercycle has been extinguished by some external event, the remaining dynamic system is unstable and approaches a pure state after long enough time. In all cases, a species will be selected which occurs just before the break in the hypercycle. In other words, species I_i will remain the last remnant of a hypercycle which has been destroyed by extinction of its constituent I_j, when i is the precursor of j ($j=i+1-\delta_{in}$). This behavior is not unexpected in light of the known properties of catalytic chains.

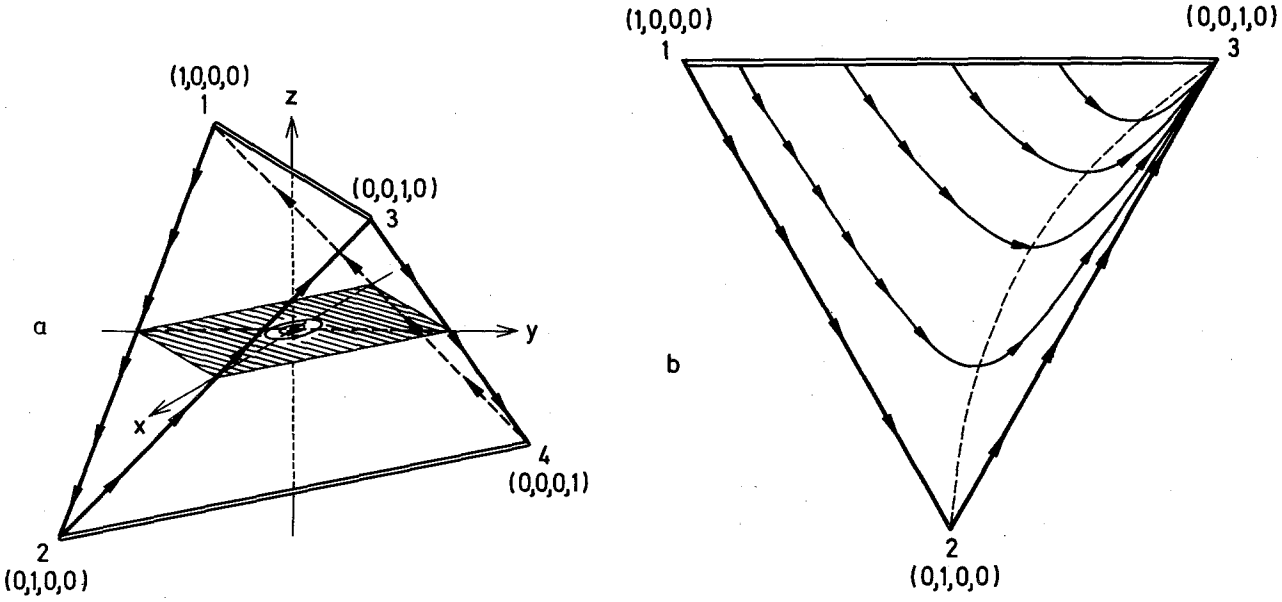

Fig. 31. Dynamic topology of the elementary hypercycle of dimension $n=4$. The dynamic system on the simplex consists of the system **4** on the interior IS_4 and four equivalent systems of type **3A** on equilateral triangles (S_3), each of which is circumscribed by two flowing edges **2A** and one fixed-point edge **2B**. a) The system on the interior is described appropriately in the variables x, y, and z (see Table 11). The manifold of closed concentric orbits belonging to the center of the linearized system lies in the x,y-plane (hatched region in the drawing). b) The dynamic system **3A**: All trajectories start out from some point on the fixed-point edge ($\overline{13}$) and end in the same corner (3). The dashed line connects all the points at which the trajectories are parallel to the fixed-point edge ($\overline{13}$)

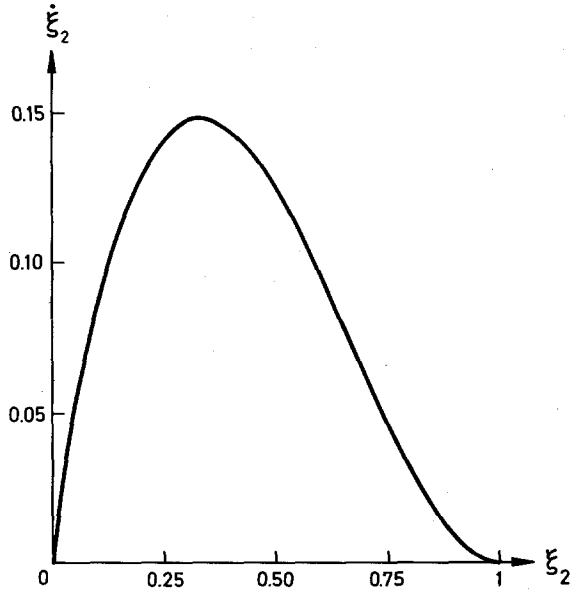

Fig. 32. The 'flowing edge' **2A**. The tangent vector $\dot{\xi}_2=\xi_2(1-\xi_2)^2$ is positive inside the whole physically allowed region ($0<\xi_2<1$) and vanishes at both ends, which represent the two fixed points of the system: $\bar{\xi}_1=(1,0)$ and $\bar{\xi}_2=(0,1)$. $\dot{\xi}_2>0$ means that ξ_2 is increasing during the next differential interval of time. Hence there is only one orbit on **2A** leading from $\bar{\xi}_1$ to $\bar{\xi}_2$, i.e., from corner 1 ($\xi_2=0$) toward corner 2 ($\xi_2=1$). The dynamic system 'flows' along this edge. Note that $d\dot{\xi}_2/d\xi_2$ vanishes at the fixed point $\bar{\xi}_2$ ($\xi_2=1$), leading to an eigenvalue $\omega=0$ in the linearized system. Consequently, fixed-point analysis fails to make a prediction about the stability of this point

VIII.2. Numerical Integration

The systems of differential equations for basic hypercycles with dimensions up to $n\leqq 12$ have been integrated by standard numerical techniques. The corresponding solution curves $\mathbf{x}(t)$ have been presented in a previous paper [4] and need not be repeated, since we are interested in a different aspect of the problem here. Our present purpose is to search for stable attractors in the interior of the simplices S_n that guarantee cooperative behavior of the constituents. For this goal an investigation of the manifold of trajectories is straightforward.

Differential equations for trajectories are obtained by elimination of the explicit time dependence in the original dynamic system:

$$\begin{aligned}
\frac{dx_2}{dx_1}&=\frac{\Lambda_2}{\Lambda_1}=f_2(x_1,x_2,\ldots,x_n)\\
\frac{dx_3}{dx_1}&=\frac{\Lambda_3}{\Lambda_1}=f_3(x_1,x_2,\ldots,x_n)\\
&\vdots\\
\frac{dx_n}{dx_1}&=\frac{\Lambda_n}{\Lambda_1}=f_n(x_1,x_2,\ldots,x_n)
\end{aligned}\qquad(70)$$

Integration of this new $(n-1)$-dimensional dynamic system yields the trajectories as solution curves:

$$\begin{aligned}
x_2&=g_2(x_1,x_2,\ldots,x_n)\\
x_3&=g_3(x_n,x_2,\ldots,x_n)\\
&\vdots\\
x_n&=g_n(x_1,x_2,\ldots,x_n)
\end{aligned}\qquad(71)$$

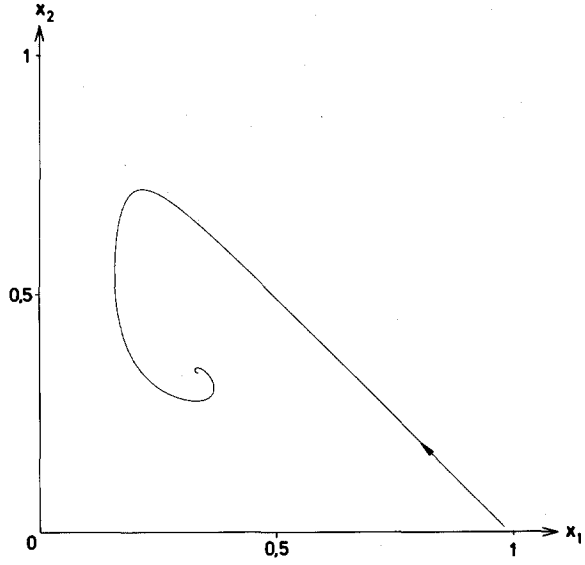

The trajectory thus is a curve in the n-dimensional concentration space. For graphical representation we shall use projections of these curves on the planes spanned by one selected coordinate x_k and by x_1. Trajectories for hypercycles of low dimension ($n=2$, 3, and 4) reflect the already known properties of these dynamic systems. The case $n=2$ is rather trivial: There are only two orbits which converge to the central stable focus (Fig. 30). The trajectories of the three-dimensional hypercycle ($n=3$) are spirals which rapidly approach the central fixed point (Fig. 33). This kind of trajectory corresponds to strongly damped oscillations of the solution curves $\mathbf{x}(t)$. The four-membered hypercycle deserves further consideration. Again, the trajectories spiral into the center of the simplex (Fig. 34a, b). In contrast to the three-dimensional example, the central force is much weaker than the rotational component. Accordingly, convergence

Fig. 33. A trajectory of the dynamic system (**3**) for the elementary hypercycle of dimension $n=3$ is shown as a projection on the plane (x_1, x_2). Initial conditions: $x_1(0)=0.98$, $x_2(0)=x_3(0)=0.01$

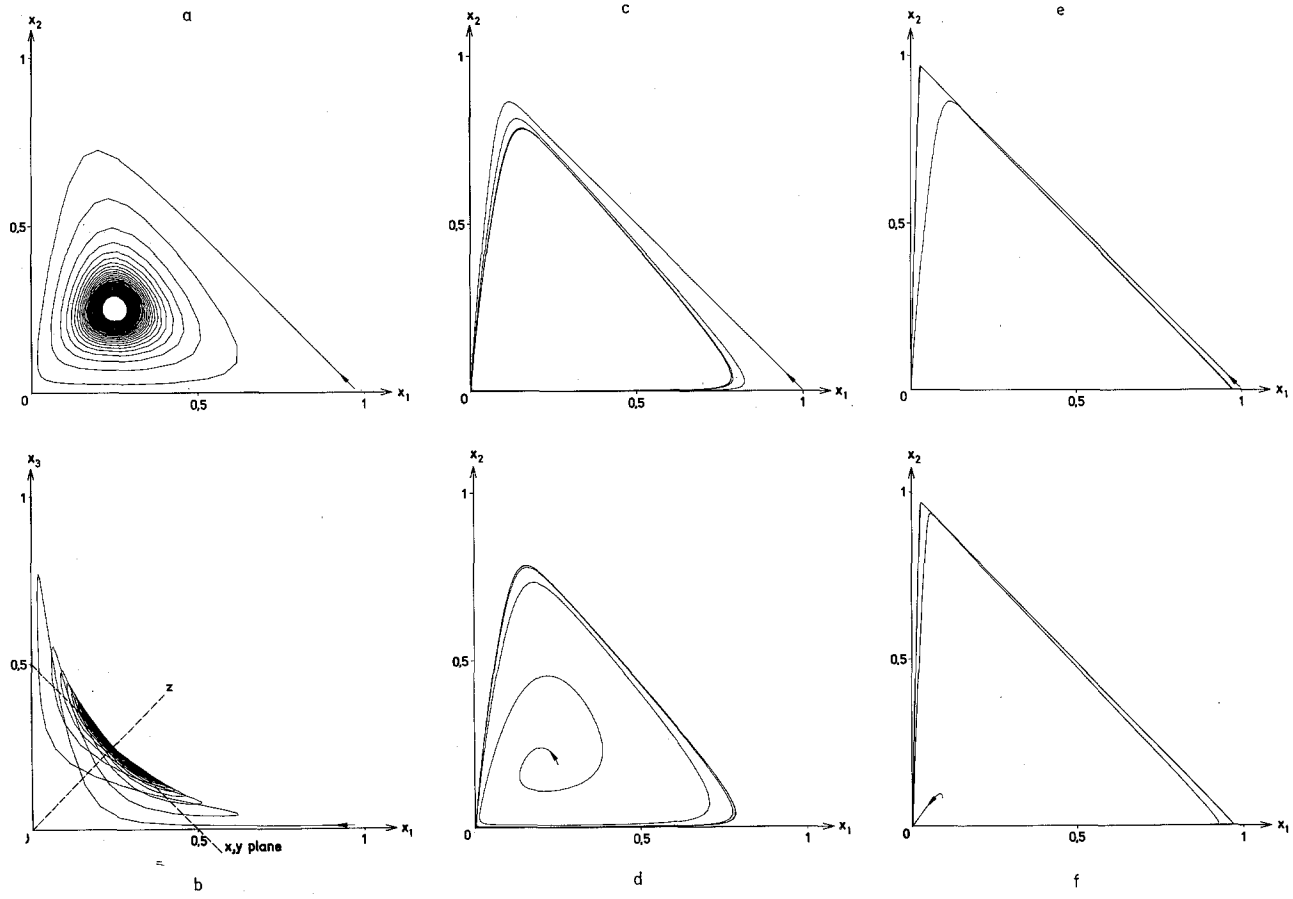

Fig. 34. Trajectories of the dynamic systems (**4**, **5**, and **12**) for elementary hypercycles of dimension $n=4$, 5, and 12, respectively. (1) $n=4$: initial conditions: $x_1(0)=0.97$, $x_2(0)=x_3(0)=x_4(0)=0.01$; two projections are shown. a) Projection of the trajectory on the plane (x_1, x_2). The trajectory spirals into the central fixed point with hardly damped oscillations. b) Projection of the trajectory on the plane (x_1, x_3). The plane of the center manifold (x, y-plane in Fig. 31) intersects the x_1, x_3-plane along the line $x_1+x_3=1/2$. Perpendicular to it we see the z-axis. Note that the trajectory crosses this plane (x, y) only at single points and does not stay therein for a longer period (Table 11). (2) $n=5$: projections on the plane (x_1, x_2). c) Initial conditions: $x_1(0)=0.9996$, $x_2(0)=x_3(0)=x_4(0)=x_5(0)=0.0001$. d) Initial conditions: $x_1(0)=0.2004$, $x_2(0)=x_3(0)=x_4(0)=x_5(0)=0.1999$. Note that the dynamic system approaches the same limit cycle from both sets of initial conditions. (3) $n=12$: projections on the plane x_1, x_2. e) Initial conditions: $x_1(0)=0.9989$, $x_2(0)=....x_{12}(0)=0.0001$. f) Initial conditions: $x_1(0)=0.0848$, $x_2(0)=....x_{12}(0)=0.0832$. Again both limit cycles are the same and come very close to the loop 12, 23 ... 11, 12, 12 1

toward the central fixed point is extremely slow. A projection of the trajectory on the x_1, x_3-plane nicely illustrates the previously derived result that there is no orbit in the plane $x_1+x_3=1/2$, $x_2+x_4=1/2$. Indeed, as one can see from Figure 34b, the trajectories follow closely a saddle-like bent surface.

For basic hypercycles of dimension $n \geqq 5$ the central fixed point represents an unstable saddle. There is no sink in the boundary and consequently one expects a stable closed orbit. The analytical techniques have not yet been developed to a sufficient extent to provide the proof of the existence of such an attractor in the interior of the simplices. Therefore, we have to rely on numerical results.

Numerical integration indeed provides strong evidence for a limit cycle or closed orbit. Starting from various points very close to the center, to a face, to an edge, or to a corner of the simplex we always arrive at the same limit cycle after long enough time. Two typical trajectories are shown in Figure 34c–f, for elementary hypercycles of dimensions $n=5$ and $n=12$, respectively. As we can see from a comparison of the two Figures, with increasing n the limit cycle approaches more closely the loop $\overline{12}, \overline{23}, \ldots, \overline{n1}$ mentioned in the previous section. Consequently the oscillations in the individual concentrations become more and more like rectangular pulses.

The use of numerical techniques also enables us to remove the assumption: $k_1=k_2 \ldots =k_n$. Calculations with arbitrary k values have been performed for dynamic systems of dimensions $n=4$ and $n=5$. No change in the general nature of the solution curves is observed. Typical examples are shown in Figures 35 and 36. The individual concentrations in both systems oscillate. For $n=4$ the concentration waves are damped and the dynamic system approaches the central fixed point. Its coordinates are determined by the following equations:

$$\bar{\mathbf{x}}_0\colon\ \bar{x}_i^0=\frac{k_j^{-1}}{\sum_{l=1}^{n} k_l^{-1}}\,c_0;\qquad j=i+1-n\delta_{in} \tag{72}$$

Five-membered hypercycles with unequal rate constants show the same kinds of undamped concentration pulses that we have observed in the system with equal k values. The size of the pulses is no longer the same for all subunits. Time-averaged concentrations [as defined by Equation (67)] fulfil the above equation (72), which determines the position of the (unstable) central fixed point. Accordingly, the pulses for those species which precede a step with a relatively small rate constant are broad, whereas those of species preceding a relatively fast reaction step are small in width and height. The system thus regulates the concentration of its constituents in such a way that the overall production rate is optimized.

Hypercycles of higher dimensions ($n \geqq 5$) do not exist in stable states with constant stationary concentrations but exhibit wave-like oscillations around an unstable fixed point in the center. Nevertheless, the constituents show cooperative behavior since their concentrations are controlled by the dynamics of the whole system and no population variable vanishes.

Dynamic systems corresponding to elementary hypercycles have one and only one attractor in the interior of the simplex, the basin of which is extended over the entire region of positive (nonzero) concentrations of all compounds. At low dimension ($n \leqq 4$) the attractor is an asymptotically stable fixed point, namely, a foxus for $n=2$ and a spiral sink for $n=3$ and $n=4$. In systems of higher dimensions ($n \geqq 5$) numerical integration provides strong evidence for the existence of a stable limit cycle. All elementary hypercycles thus are characterized by cooperative behavior of their constituents.

Due to their dynamic features hypercycles of this type hide many yet unexplored potentialities for self-organization (dissipative structures, e.g., in case of superimposed transport). They may also play an important role in the self-organization of neural networks.

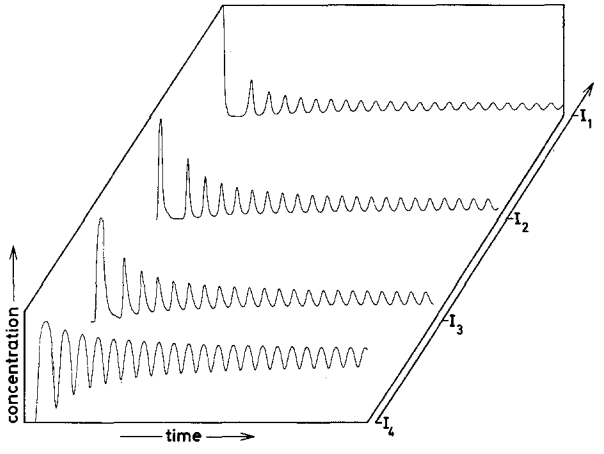

Fig. 35. Solution curves of the dynamic system for an elementary hypercycle with dimension $n=4$ and unequal rate constants ($k_1=0.25$, $k_2=1.75$, $k_3=1.25$, $k_4=0.75$; initial conditions: $x_1(0)=0.9997$, $x_2(0)=x_3(0)=x_4(0)=0.0001$; full concentration scale = 1 concentration unit, full time scale = 1000 time units). Note that the concentration of I_1 (the component preceding the fastest step) is smallest whereas that of I_4 (the component before the slowest step) is largest

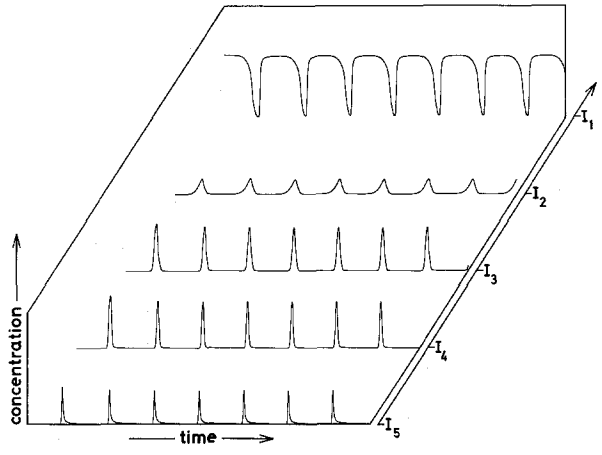

Fig. 36. Solution curves of the dynamic system for an elementary hypercycle with dimension $n=5$ and unequal rate constants ($k_1=25/13$, $k_2=1/13$, $k_3=19/13$, $k_4=1$, $k_5=7/13$; initial conditions: $x_1(0)=0.9996$, $x_2(0)=x_3(0)=x_4(0)=x_5(0)=0.0001$; full concentration scale = 1 concentration unit, full time scale = 1000 time units). Note that the concentration of I_5 (the component before the fastest step) is smallest, whereas that of I_1 (the component before the slowest step) is largest

IX. Hypercycles with Translation

IX.1. Ideal Boundary Conditions and General Simplifications

An appropriate set of boundary conditions can be realized in a flow reactor [4, 9, 55, 56]. The concentrations of all low-molecular-weight compounds (m_i, $i=1,2,\ldots,\lambda$) are buffered with the help of controlled flow devices, at the same time providing the energy supply for the system. The concentration variables x_i refer to the macromolecular species synthesized in the reactor, while all other compounds of the 'standard reaction mixture' do not show up explicitly in the differential equations, but appear implicitly in the effective rate constants of Equation 30.

Because of technical difficulties and also for heuristic reasons it is impossible to account explicitly for all elementary steps in the reaction mechanism. We rather have to apply simplified reaction schemes which lead to an appropriate 'over-all' kinetics. This strategy is a common procedure in chemical kinetics. Acid base reactions in aqueous solution for example are generally described by phenomenologic equations which do not account for individual proton jumps, but just reflect changes in protonation states of the molecules considered.

For the mechanism of template-directed polymerization and translation, the rate equations contain the population numbers of the complete macromolecules as the only variables. Hence chain initiation and propagation steps are not considered explicitly. A justification for these approximations can be taken from experiments. Actually, the kind of 'over-all' kinetics we are using here is well established (cf. Part C).

IX.2. The Kinetic Equations

The catalytic hypercycle shown schematically in Figure 37 consists of two sets of macromolecules: n polynucleotides and n polypeptides. The replication of polynucleotides (I_i) is catalyzed by the polypeptides (E_i) which, in turn, are the translation products of the former. The hypercyclic linkage is established by two types of dynamic correlations:

1. Each polynucleotide I_i is translated uniquely into a polypeptide E_i. The possibility of translation evidently requires the existence of an appropriate machinery which is composed of at least some of the translation products E_i and which uses a defined genetic code.
2. Polynucleotides and polypeptides form specific complexes that are also catalytically active in the synthesis of polynucleotide copies. The polypeptides may be specific replicases or specific cofactors of a common protein with polymerase activity. Altogether these primordial proteins provide at least two functions: specific replication and translation. How such a system can be envisaged is shown in Part C.

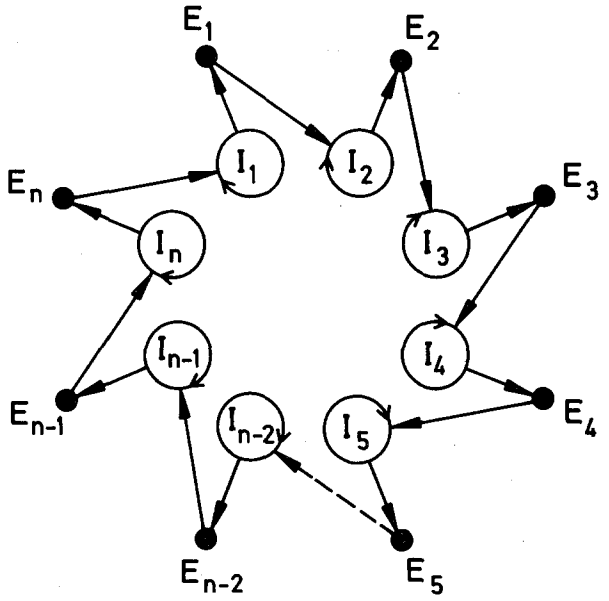

Fig. 37. Schematic diagram of a hypercycle with translation. Dimension: $2\times n$, i.e., n polynucleotides and n polypeptides

The couplings between the I_i and E_i have to be of a form which allows the closure of a feedback loop (Fig. 37). In mathematical terms cyclic symmetry is introduced by assuming specific complex formation between the enzyme E_j and the polynucleotide I_i, whereby $j=i+1-n\delta_{in}$.

The kinetics of polynucleotide synthesis follows a Michaelis-Menten-type reaction scheme, although we do not introduce the assumption of negligibly small complex concentrations.

$$I_i+E_j \overset{K_i}{\rightleftharpoons} I_iE_j; \quad I_iE_j+\sum \nu_\lambda^I M_\lambda^I \overset{f_i}{\rightarrow} I_i+I_iE_j \tag{73}$$

The four nucleotide triphosphates and their stoichiometric coefficients are denoted by M_λ^I and ν_λ^I; $\lambda=1,2,3,4$, respectively. Now we introduce z_i for the concentration of the complex I_iE_j and x_j^0, y_i^0 or x_j, y_i for the total or free concentrations of polypeptides (E_j) and polynucleotides (I_i). Mass conservation requires:

$$x_j^0=x_j+z_i \quad \text{and} \quad y_i^0=y_i+z_i \tag{74}$$

For fast equilibration of the complex the concentration z_i is related to the total concentrations x_j^0 and y_i^0 as:

$$z_i=\frac{y_i^0+x_j^0+K_i}{2}\left(1-\sqrt{\frac{4y_i^0x_j^0}{(y_i^0+x_j^0+K_i)^2}}\right) \tag{75}$$

Polypeptide synthesis is assumed to be unspecific, i.e., translation of the polynucleotide I_i occurs with the help of a common 'apparatus':

$$I_i+\sum_\lambda \nu_\lambda^E M_\lambda^E \overset{k_i}{\rightarrow} I_i+E_i \tag{76}$$

M_λ^E and ν_λ^E denote the activated amino acids and their stoichiometric coefficients, respectively. Selection constraints may be introduced properly by controlling total concentrations for both kinds of biopolymers (I and E) independently. By analogy with the constraints of constant organization we keep both sums of concentrations constant:

$$\sum_k y_k^0 = c_I^0; \quad \sum_k x_k^0 = c_E^0 \tag{77}$$

Under all these conditions our dynamic system consiting of $2n$ coupled differential equations reads:

$$\begin{aligned} \dot{y}_i^0 &= f_i z_i - \frac{y_i^0}{c_I^0} \sum_{k=1}^{n} f_k z_k \\ \dot{x}_i^0 &= k_i y_i - \frac{x_i^0}{c_E^0} \sum_{k=1}^{n} k_k y_k \\ i &= 1, 2, \ldots, n. \end{aligned} \tag{78}$$

For our purpose, it is sufficient to discuss two limiting cases:

1. The concentration z_0 of the complex $I_i E_j$ becomes proportional to the product of polynucleotide and polypeptide concentrations at sufficiently low concentrations:

$$y_i^0, x_j^0 \ll K_i; \quad z_i \sim \frac{1}{K_i} y_i^0 x_j^0; \quad z_i \ll y_i^0, x_j^0 \tag{79}$$

If we further assume the first-order translation process to be fast as compared to the second-order replication – an assumption that is well justified, at least for low concentrations of polynucleotides – the polypeptide concentration will assume a stationary value that can be included in the rate parameters. The formation of polynucleotides then is described by a system of differential equations that is typical of an elementary hypercycle of dimension n.

2. At high concentrations, z_i becomes equal to the smaller of the two variables:[3]

$$z_i = \inf(y_i^0, x_j^0) \tag{80}$$

Accordingly, we approach two possible limiting situations

$$K_i \ll y_i^0 \ll x_j^0: \; z_i \sim y_i^0 \tag{81}$$

$$K_i \ll x_j^0 \ll y_i^0: \; z_i \sim x_j^0 \tag{82}$$

In the first of these two cases the polynucleotides behave like independent competitors, while the polypeptides – due to $y_i = y_i^0 - z_i \approx 0$ – remain stationary. Under natural conditions, where constraints like 'constant total concentrations' usually do not apply – at least not for the assumed small values of y – the resulting growth of polynucleotides would lead to a reversal of the concentration ratios $y{:}x$ and hence to an approach to condition (82). As a consequence, the approximations

$$z_i \approx x_j^0 \quad \text{and} \quad y_i \approx y_i^0 \tag{83}$$

become valid, leading to a $2n$-membered catalytic cycle, but not a hypercycle. Thus under saturation conditions, i.e., at high concentrations of the constituents, the hypercycle loses the behavior typical of nonlinear growth rates. As a unified system it simulates the properties of a simple catalytic cycle, which is equivalent to an autocatalyst or self-reproducing unit.

IX.3. Numerical Solutions

The differential equations derived for catalytic hypercycles with explicit consideration of complex formation between the polynucleotides and polypeptides are difficult to study by analytical methods, because of the irrational expressions involved. Numerical integration is time-consuming in these cases, but nevertheless, it represents the only source of information on the properties of these dynamic systems. To illustrate the dynamics of polynucleotide–polypeptide hypercycles we shall present computer graphs of solution curves as well as trajectories.

In comparison to elementary hypercycles the polynucleotide–polypeptide systems contain a new class of parameters, namely, the association constants of the complexes, K_i. As to be expected from the differences in kinetic behavior at the low and high concentration limits, the equilibrium constants exhibit a dominating influence on the dynamic properties of the system. For the sake of a systematic investigation we reduce the number of independent parameters. The assumptions made are essentially the same as those used for the elementary hypercycles: All rate constants for polynucleotide replication, $f_1 = f_2 = \cdots f_n = f$, for their translation into polypeptides $k_1 = k_2 = \cdots = k_n = k$, and all association constants, $K_1 = K_2 = \cdots = K_n = K$ are assumed equal. Then, we study the influence of K on the properties of the dynamic systems at fixed values of f and k and for a constant set of initial concentrations. For hypercycles of dimensions $n \leqq 4$ the solution curves approach a stable stationary state after long enough time. The individual concentrations may exhibit damped oscillations. The dynamics of these systems are essentially the same as for hypercycles with higher values of n and small equilibrium constants.

The dynamics of higher-dimensional hypercycles are more complicated. The long-term behavior of the system changes with increasing values of the equilibrium constant K. Below a certain critical value (K_{cr}) the system converges toward stable stationary states,

[3] inf = infimum is the mathematical term representing the smallest member of a set.

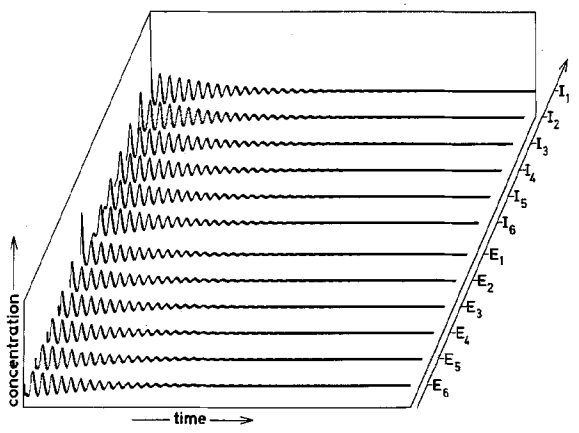

Fig. 38. Solution curves of the dynamic system for a hypercycle with translation. Dimension: 2×6, $k=0.25$; initial conditions: $y_1(0)=5.0$, $y_2(0)=\cdots=y_6(0)=0.5$; $x_1(0)=\cdots=x_6(0)=1.0$; full concentration scale = 5 concentration units, full time scale = 1000 time units. The value of the equilibrium constant K is below the critical value for the Hopf bifurcation and hence a damped oscillation is observed

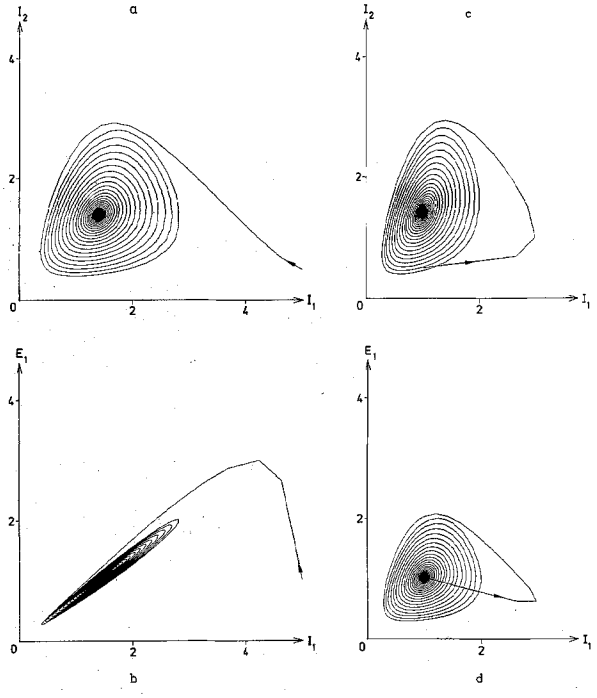

Fig. 39. A trajectory of the dynamic system for a hypercycle with translation. Dimension: 2×5, $k=1.0$; initial conditions: $y_1(0)=5.0$, $y_2(0)=y_3(0)=y_4(0)=y_5(0)=0.5$; $x_1(0)=x_2(0)=x_3(0)=x_4(0)=x_5(0)=1.0$. a) Projection of the trajectory on the plane (y_1, y_2) showing the concentrations of the polynucleotides I_1 and I_2. b) Projection on the plane (y_1, x_1) showing the concentrations of the polynucleotide I_1 and its translation product, the enzyme E_1. Note that the concentration of E_1 is roughly proportional to that of I_1 and thus the condition for simplifying the hypercycle with translation is fulfilled to a good approximation. c) Projection on the plane (x_1, y_2) showing the concentrations of the polypeptide E_1 and the polynucleotide I_2, the formation of which is catalyzed by the former. d) Projection on the plane (x_1, x_2) showing the concentrations of the polypeptides E_1 and E_2. Note that K again is below the critical value of the Hopf bifurcation and the trajectory converges to the central fixed point

whereas limit cycles are obtained for larger values of $K(K > K_{cr})$. According to the appearance of solution curves and trajectories we distinguish four different cases, arranged with respect to increasing values of the equilibrium constant K:

1. At small values of K the dynamic behavior is qualitatively the same as of hypercycles of lower dimensions. The solution curves exhibit strongly dampled oscillations (Fig. 38) and the trajectories spiral quickly into the center, which represents a stable stationary state (Fig. 39).

2. In principle we find the same general type of dynamic behavior as in case (1). The oscillations, however, are damped only slightly and the approach toward the stationary state is extremely slow (Fig. 40a, b). The situation is quite different from case (1), because the damping terms do not show up in normal mode analysis but require consideration of nonlinear contributions. Phenomenologically this fact reveals itself in the appearance of initially (almost) constant amplitudes of oscillation. This situation occurs at values of the equilibrium constant K that are slightly smaller than the critical value K_{cr}, i.e.: $K = K_{cr} - \delta K$.

3. At values of K that are slightly larger than the critical equilibrium constant $(K = K_{cr} + \delta K)$, we observe an interesting phenomenon. The dynamic system first behaves much as in case (2). The individual concentrations oscillate with relatively small amplitudes. In contrast to case (2), the amplitudes increase slightly during the initial period. After this phase of sinusoidal oscillation, however, the concentration waves change abruptly in shape and frequency (Fig. 40c, d) and then resemble closely the rectangular pulses which we encountered in basic hypercycles of high dimension. Finally, the dynamic system approaches a limit cycle.

4. At large values of K the individual concentrations oscillate with increasing amplitude and the dynamic system steadily approaches the limit cycle (Fig. 40e, f). The kind of change in dynamic behavior with a continuously varying parameter as we have observed here is known in the literature as 'Hopf bifurcation' [58]. The characteristic retardation in convergence toward the long-term solution that we have found in cases (2) and (3) has been described also for other dynamic systems and is usually called the 'critical slowing down' at the Hopf bifurcation. In the case of hypercycles, the 'slowing down' around the critical value of K becomes more pronounced at larger values of n. In the five-membered cycle $(n=5)$ a situation corresponding to case (3) is hardly detectable. The catalytic hypercycle with $n=10$, on the other hand, shows a much longer initial period, as referred to in case (3), than the six-membered system (Fig. 41). The initial

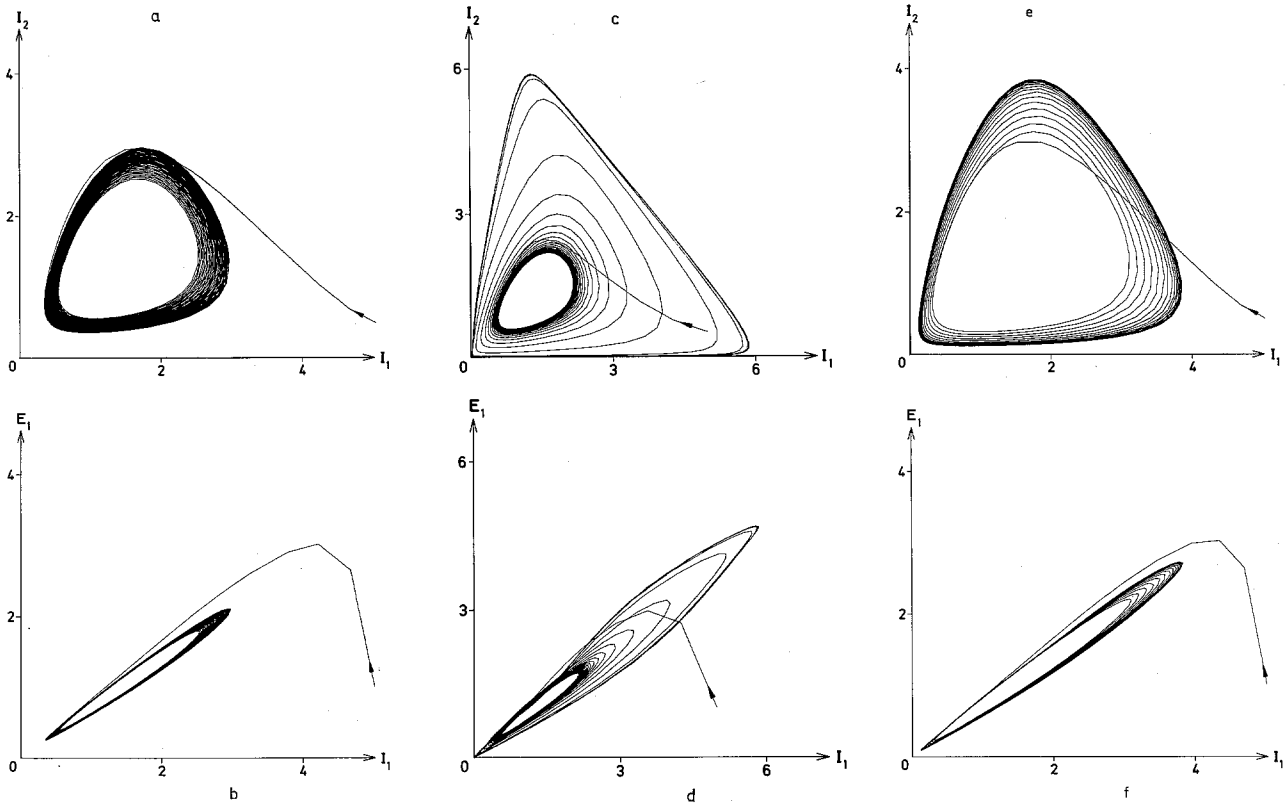

Fig. 40. Trajectories of the dynamic systems for hypercycles with translation. a and b) Dimension 2×5, $K = 1.1$, initial conditions: $y_1(0) = 5.0$, $y_2(0) = y_3(0) = y_4(0) = y_5(0) = 0.5$; $x_1(0) = x_2(0) = x_3(0) = x_4(0) = x_5(0) = 1.0$; projections are shown on the planes for the concentrations of I_1, I_2, and I_1, E_1, respectively; the value of the equilibrium constant K is slightly below the Hopf bifurcation and we observe very slow convergence toward the stable central fixed point. c and d) Dimension 2×6, $K = 0.2784$, initial conditions: $y_1(0) = 5.0$, $y_2(0) = \cdots = y_6(0) = 0.5$, $x_1(0) = \ldots x_6(0) = 1.0$; projections are shown on the planes for the concentrations of I_1, I_2, and I_1, E_1, respectively; the value of the equilibrium constant K is slightly above the Hopf bifurcation and we observe a metastable limit cycle before the system finally converges to the stable limit cycle. e and f) Dimension 2×5, $K = 1.2$, initial conditions: $y_1(0) = 5.0$, $y_2(0) = y_3(0) = y_4(0) = y_5(0) = 0.5$, $x_1(0) = x_2(0) = x_3(0) = x_4(0) = x_5(0) = 1.0$; projections are shown on the planes for the concentrations of I_1, I_2, and I_1, E_1, respectively; the value of the equilibrium constant K is above the Hopf bifurcation and the system converges steadily toward the stable limit cycle. Note that the proportionality between E_1 and I_1 is reasonably well fulfilled in all three cases (b, d and f)

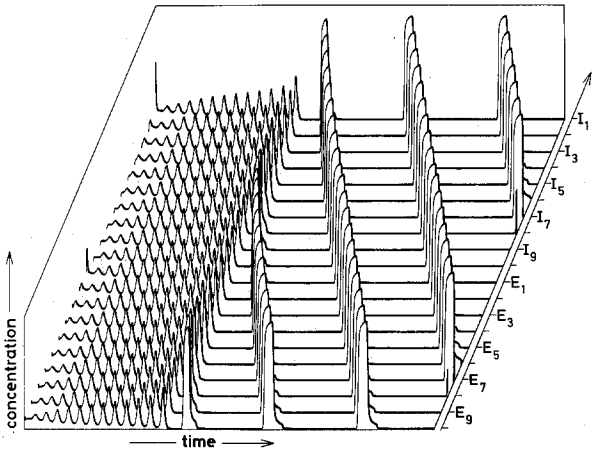

Fig. 41. Solution curves of the dynamic system for a hypercycle with translation. Dimension 2×10, $K = 0.026$; initial conditions: $y_1(0) = 5.0$, $y_2(0) = \cdots = y_{10}(0) = 0.5$; $x_1(0) = \cdots = x_{10}(0) = 1.0$; full concentration scale = 10 concentration units, full time scale = 1000 time units. The value of the equilibrium constant chosen is slightly above the critical value for the Hopf bifurcation. We observe a metastable oscillatory state which changes suddenly into the final limit cycle with the characteristic concentration waves

phase of sinusoidal oscillations resembles a metastable oscillatory state. The transition to the final limit cycle becomes sharper with increasing value of n and is quite pronounced for the ten-membered hypercycle.

All polynucleotide-polypeptide hypercycles studied so far have an attractor in the interior of the physically accessible range of concentrations. They are characterized by cooperative behavior of their constituents. Depending on the values of the product of total concentrations (c_0^N and c_0^P) and of association constants (K) as well as on the size of the hypercycles, we observe stable fixed points or limit cycles. Small K values then are complementary to high concentrations and *vice versa*. The long-term behavior at low and high concentration limits, obtained by numerical integration, agrees completely with the predictions based on the analysis given in the last section. One of the basic simplifications, which concerned quasi-stationarity of polypeptide synthesis, can be checked directly by an inspection of the projections of trajectories onto the E_1,

I_1 plane. For the stationary-state approximation we expect to find straight lines. As we can see from Figures 39b and 40b, d, f, proportionality of the two concentrations is roughly fulfilled and the simplified treatment appears to be well justified. It was, actually, the purpose of the numerical analysis of this complex reaction mechanism to verify the equivalence of complex and elementary hypercycles as far as their self-organizing properties are concerned. The conclusions reached with elementary systems therefore are relevant also for all kinds of realistic hypercycles of a more complex structure (cf. Part C).

X. Hypercyclic Networks

X.1. Internal Equilibration and Competition between Hypercycles

The concept of internal equilibration as introduced in Section VI seems to be very useful for a straightforward analysis of more complex networks since it permits a reduction of the number of independent variables.

At first we investigate the process of equilibration in basic hypercycles. For that purpose we calculate time averages of the individual concentrations $X_i(t)$ – see Equation (67) and compare them with the corresponding solution curves $x_i(t)$ (Fig. 42). No matter whether the final state is stationarily inert or oscillating, the time averages $X_i(t)$ become practically constant after a few cycles. The assumption of established internal equilibrium therefore seems to be a well-justified approximation for hypercycles. Nevertheless, we shall check it in a few cases.

Using the concept of internal equilibration we can derive an equation for the net growth rate of entire hypercycles:

$$\dot{c}=\sum_{i=1}^{n}\dot{x}_i=\sum_{i=1}^{n}\Gamma_i(\mathbf{x})=\sum_{i=1}^{n}k_i x_i x_j$$
$$=\frac{1}{\sum_{i=1}^{n}k_i^{-1}}\,c^2\equiv\bar{k}c^2=\Gamma(c) \qquad (84)$$
$$j=i+1-n\delta_{in}$$

Hypercycles, thus, are characterized by quadratic growth rates and follow a hyperbolic growth law. They represent appropriate examples for the kind of non-Darwinian 'once-for-ever' selection discussed in Sections VI and VII.

According to the expression for $\bar{k}$ in Equation (84) the rate constant of an entire hypercycle will be of the same order of magnitude as that of its slowest single step. Under the condition of unlimited growth, hypercycles grow hypothetically to infinity at a certain critical time (t_∞). In fully equilibrated systems these instabilities occur at

$$t_\infty^e=[kc(t=0)]^{-1} \qquad (85)$$

The results for equilibrated hypercycles calculated from Equation (85) are compared with the values obtained by numerical integration of systems far off internal equilibrium (t_∞^n) in Table 12. In fully equilibrated systems the instabilities always occur somewhat earlier, $t_\infty^e<t_\infty^n$. On the whole, these numerical differences are of minor importance only, the general behavior of the dynamic systems and the relative values of t_∞ being predicted correctly. The assumption of internal equilibration thus appears to be a good approximation for most nonequilibrated systems.

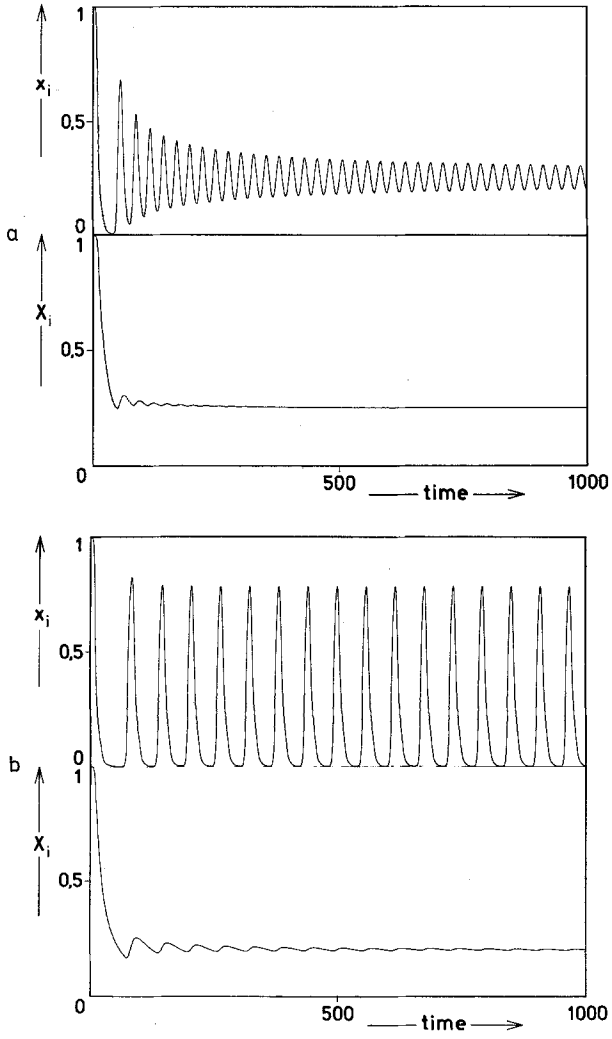

Fig. 42. Solution curves of the dynamic systems for elementary hypercycles of dimension $n=4$ and $n=5$ with equal rate constants and time-averaged concentrations $X(t)$; (a) $n=4$ and b) $n=5$. Note that $X(t)$ reaches $\bar{X}$ after a few oscillations, i.e., internal equilibrium is established relatively fast in both examples

Naturwissenschaften 65, 7–41 (1978)

Table 12. Instabilities in the dynamic systems for hypercycles under unlimited growth conditions

Dimension	Boundary and initial conditions			Critical time constants	
	Rate constant	Initial concentration	Initial distribution[a]	At equilibrium	Far off equilibrium
n	k	$c(0)$	$\mathbf{x}(0)$	t^e_∞	t^n_∞
2	$\frac{1}{2}$	0.55	(0.5, 0.05)	3.64	5.0
3	$\frac{1}{3}$	0.60	(0.5, 0.05, 0.05)	5.00	6.8
4	$\frac{1}{4}$	0.65	(0.5, 0.05, 0.05, 0.05)	6.15	7.3

[a] The distribution of initial concentrations applied in the numerical integration of the system far off equilibrium $\mathbf{x}(0)=(x_1(0), x_2(0)\ldots)$.

Selection among entire hypercycles as single entities can be studied generally under the assumption of internal equilibrium. The dynamic systems obtained thereby are, of course, identical with those describing independent competitors that are characterized by quadratic growth rates. Competition between non-equilibrated hypercycles is more difficult to investigate, since only numerical integration of the systems of differential equations is possible. An example has been treated elsewhere [53], demonstrating that the assumption of internal equilibration represents a powerful approximation.

As an example for competing systems we consider the two hypercycles H_A and H_B with n_A and n_B members subject to the constraints of constant organization.
If there is internal equilibration the system reduces to two competitors with quadratic growth-rate terms. From the results of fixed-point analysis we recall that hypercycle H_A will be selected when its relative initial concentration $c_A(0)$ exceeds a critical limit:

$$\lim_{t\to\infty} c_A(t)=c_0 \quad \text{if } c_A(0)>\frac{k_B}{k_A+k_B}c_0 \tag{86}$$

Otherwise hypercycle H_B wins the competition.
It seems illustrative to consider one more special case. We assume the individual rate constants to be very similar within a given hypercycle, i.e., $k_1\sim k_2\sim\cdots\sim k_n=\bar{k}_A$ and $k_{n+1}\sim k_{n+2}\sim\cdots\sim k_{n+m}=\bar{k}_B$. Then the rate constants for entire hypercycles are obtained as follows:

$$k_A=\frac{1}{n_A}\bar{k}_A \quad \text{and} \quad k_B=\frac{1}{n_B}\bar{k}_B \tag{87}$$

As we see, the constants are inversely proportional to the numbers of members in the hypercycle and consequently, smaller cycles seem to have a certain selective advantage. If we assume, however, all macromolecules to be present at roughly the same concentrations ($\bar{x}$), the disadvantage of the larger cycle is compensated exactly by a larger value of the total concentration, c:

$$\begin{aligned} &c_A(0)=n_A\cdot\bar{x}, \quad c_B(0)=n_B\cdot\bar{x} \quad \text{and} \quad c_0=(n_A+n_B)\bar{x} \\ &\lim_{t\to\infty} c_A(t)=c_0 \quad \text{if } \bar{k}_A>\bar{k}_B \end{aligned} \tag{88}$$

Therefore, the chance of survival is roughly the same for hypercycles of different sizes or dimension n, provided the initial concentrations of the individual members and the rate constants for the replication steps are equal.
The results obtained for two hypercycles can be generalized easily to N independent competitors.

XI.2. Parasitic Coupling and Catalytic Networks

The cyclically closed catalytic link, which connects all active members $I_1 \ldots I_n$ of a hypercycle might include branching points and thereby provide a furthering of external species $I_{k\neq 1\ldots n}$, not being an intrinsic part of the cooperative unit. We call these external members parasites. To make an analytical treatment feasible we shall assume internal equilibrium within the cycle (Table 13). Two dynamic systems describing a hypercycle and a single-membered parasite have been investigated by the fixed-point method.
The first example is represented by a catalytic hypercycle and a parasite that is not capable of self-replication (Fig. 43a). Above a certain threshold value of total concentration ($k_A c_0 > k$), as we can see from Table 13, hypercycle and parasite are present with nonzero concentration at the stationary state. The equilibrium concentration of the hypercycle grows with increasing c_0, whereas the concentration of the parasite remains constant. At high enough concentration, consequently, the parasite will lose its importance for the dynamics of the cycle completely. At low total concentration ($k_A c_0 < k$) the system becomes unstable. Within the limits of the assumption of internal equilibrium the parasite destroys the hypercycle and finally represents the only remnant of the dynamic system.
The second case describes the development of a hypercycle with a self-replicative parasite attached to it (Fig. 43b). This dynamic system is characterized by sharp selection depending on the relative values of the rate constants k and k_A. For $k > k_A$ the parasite destroys the hypercycle whereas the inequality $k < k_A$ implies that the parasite dies out. It might be of some interest to consider the dynamic system explicitly on the level of individual polynucleotides. From Table 13 we obtain

$$k=k_x\frac{x_v}{c_A}=k_x\frac{k_{v+1}^{-1}}{\sum_i k_i^{-1}} \tag{89}$$

under the condition of established internal equilibrium. Using the previously derived expression

$$k_A=\left(\sum_i k_i^{-1}\right)^{-1}$$

we find:

$$k<k_A \rightarrow \frac{k_x}{k_{v+1}} \cdot \frac{1}{\sum_i k_i^{-1}} < \frac{1}{\sum_i k_i^{-1}} \rightarrow k_x < k_{v+1} \tag{90}$$

Thus the result of selection is determined completely by the ratio of the two rate constants for the reaction steps starting out at the branching point, no matter what the values of the other rate constants in the hypercycle are.

Numerical integration of dynamic systems of the types shown in Figure (43) has been performed in order to study the influence of deviations from the equilibrium distribution. In fact all the conclusions drawn here can also be verified for systems far off equilibrium.

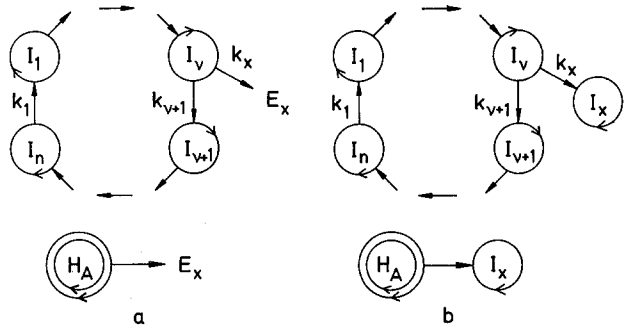

Fig. 43. Schematic diagrams for hypercycles with parasitic units, a) the parasite is not self-reproductive, b) the parasite is self-reproductive. The branching is assumed to occur at the component (I_v)

Table 13. Fixed-point analysis of hypercycles with parasitic couplings

A hypercycle with a parasitic unit I_x attached to it (Fig. 43) is described by $n+1$ differential equations, n of which are identical with those of the isolated hypercycle. For the $(n+1)$-th differential equation, which defines the concentration of the parasite, we obtain: $[I_x]=x$, $[I_v]=x_v$,

$$\dot{x}=k_x x_v-\frac{x}{c_0}\phi \tag{T.13.1}$$

for the system depicted in Figure 43a and

$$\dot{x}=k_x x_v x-\frac{x}{c_0}\phi \tag{T.13.2}$$

for the one exemplified in Figure 43b.
If an equilibrium is established within the hypercycle then the $n+1$ differential equations reduce to two. Here the introduction of new rate constants turns out to be appropriate:

$$k=k_x\cdot\frac{x_v}{c_A}:\ c_A=\sum_{j=1}^{n} x_j \tag{T.13.3}$$

and k_A as defined in Equation (84).
(1) The parasite is not self-reproductive (cf. Fig. 43a):

$$\dot{c}_A=k_A c_A^2-\frac{c_A}{c_0}(k_A c_A^2+k c_A);\quad c_0=c_A+x \tag{T.13.4}$$

$$\dot{x}=k c_A-\frac{x}{c_0}(k_A c_A^2+k c_A)$$

This dynamic system has two fixed points:

$$\bar{\mathbf{x}}_1:\ \bar{c}_A=\frac{k_A c_0-k}{k_A},\quad \bar{x}=\frac{k}{k_A} \tag{T.13.5}$$

$$\omega^{(1)}=-\frac{(k_A c_0-k)^2}{k_A}$$

$$\bar{\mathbf{x}}_2:\ \bar{c}_A=0,\quad \bar{x}=c_0;\quad \omega^{(2)}=0 \tag{T.13.6}$$

$\bar{\mathbf{x}}_1$ is stable unless the total concentration meets the critical condition $c_0=k/k_A$.
Stability analysis of $\bar{\mathbf{x}}_2$ requires a detailed inspection of the higher-order terms. For a point $x=c_0-\delta x$ we find

$$\dot{x}=\frac{(\delta x)^2}{c_0}(k-k_A c_0+k_A\delta x) \tag{T.13.7}$$

which leads to

$\dot{x}>0$ for $c_0<k/k_A$

and

$\dot{x}<0$ for $c_0>k/k_A$.

Thus, the fixed point $\bar{\mathbf{x}}_2$ is stable at concentrations below the critical value and unstable above it. At low concentrations $\bar{\mathbf{x}}_1$ lies outside the physically accessible range, $\bar{x}=c_0$ is the only stable stationary state, and the hypercycle is destroyed by the parasite. At high concentrations the stable fixed point $\bar{\mathbf{x}}_1$ lies on the simplex S_2, which means that hypercycle and parasite are coexistent.
(2) The parasite is self-reproductive (Fig. 43b):

$$\dot{c}_A=k_A c_A^2-\frac{c_A}{c_0}(k_A c_A^2+k c_A x),\quad c_0=c_A+x$$

$$\dot{x}=k c_A x-\frac{x}{c_0}(k_A c_A^2+k c_A x) \tag{T.13.8}$$

The system has two fixed points at the corners of S_2:

$$\bar{\mathbf{x}}_1:\ \bar{c}_A=c_0,\quad \bar{x}=0,\quad \omega^{(1)}=(k-k_A)c_0 \tag{T.13.9}$$

$$\bar{\mathbf{x}}_2:\ \bar{c}_A=0,\quad \bar{x}=c_0,\quad \omega^{(2)}=0 \tag{T.13.10}$$

The first fixed point is stable, provided that $k_A>k$. For the second fixed point it is again necessary to check the higher-order terms. At $x=c_0-\delta x$ we find

$$\dot{x}=\frac{k-k_A}{c_0}(\delta x)^2(c_0-\delta x) \tag{T.13.11}$$

which now leads to

$\dot{x}>0$ for $k>k_A$

and

$\dot{x}<0$ for $k<k_A$.

Thus, $\bar{\mathbf{x}}_2$ is stable if the inequality $k>k_A$ holds. The system is competitive, which signifies that hypercycle and parastic unit cannot coexist except in the special situation where the rate constants are equal $(k=k_A)$.

The results obtained for single-membered parasites can be extended to arbitrary chains using the results derived in Section VII.6. In general, the fate of the entire parasite is strongly coupled to the development of the species attached to the cycle: The parasite will die out always when the concentration of the species after the branching point approaches zero. There is one interesting special case: $k_x = k_{\nu-1}$. The differential equations for $I_{\nu+1}$ and I_x are identical and hence the ratio of the two species always remains constant at its initial value. Numerical integration of several dynamic systems of this type showed that in this special situation ($k_x = k_{\nu+1}$) all members of the parasite besides the species I_x will die out.
Chain-like parasites might fold back on the hypercycle, thereby leading toward a catalytic network with a branching point and a confluent. By numerical integration we found that systems of these types are unstable: The less efficient branch, i.e., the branch with the smaller values of the rate constants k dies out and a single, simple hypercycle remains.

Allowing for arbitrary assignment of catalytic coupling terms to a set of self-reproductive macromolecules we shall encounter highly branched systems or complicated networks much more frequently than regular hypercycles. It is of great importance, therefore, to know the further development of these systems in order to make an estimate of the probabilities of hypercycle formation. Analytical methods usually cannot be applied to this kind of system and hence we have to rely on the results of numerical techniques.
Some general results have been derived from a variety of solution curves obtained by numerical integration of the differential equations for various catalytic networks. As suggested by the previous examples, these systems are not stable and disintegrate to give smaller fragments. Apart from complicated dynamic structures, which owe their existence to accidental coincidence of the numerical values for different rate constants, the only possible remnants of catalytic networks of self-replicative units are independently growing species, catalytic chains, or catalytic hypercycles. Thus any catalytic network consisting of self-replicative units with uniform coupling terms will disintegrate either to yield a hypercycle which then is superior to the other fragments or to give competitive dynamic systems that are not suited for cooperative evolution.

XI.3. Hierarchy of Coupling Between Hypercycles

In principle, hypercycles may be coupled to yield more highly organized systems by introduction of appropriate catalytic terms into the rate equation. We consider two basic hypercycles H_A and H_B and assume that the hypercycle H_A produces a catalytic growth factor for H_B and *vice versa*. Such a growth factor might be a constituent of the hypercycle or a substance produced by it. From our previous experience we would expect that mutual catalytic enhancement will lead to cooperative behavior.
To simplify a straightforward analysis, we assume internal equilibrium to be established in both hypercycles. The catalytic terms are of third order with respect to molecular concentrations ($k_A c_A^2 c_B$ and $k_B c_A c_B^2$, respectively, see also Table 14). Consequently, we may neglect the second-order growth functions of the uncatalyzed system at high enough concentrations. Fixed-point analysis is not sufficient to study the dynamic system obtained, since it yields zero eigenvalues for all normal modes. The vector field, however, can be investigated easily because the system has only one

Table 14. Fixed-point analysis of catalytically coupled hypercycles H_A and H_B

(1) Coupling terms of third order:

$$\dot{c}_A = k_A c_A^2 c_B - \frac{c_A}{c_0}\phi; \quad \phi = (k_A c_A + k_B c_B) c_A c_B$$

$$\dot{c}_B = k_B c_A c_B^2 - \frac{c_B}{c_0}\phi; \quad c_0 = c_A + c_B \qquad \text{(T.14.1)}$$

Fixed-point analysis of the dynamic system yields:

$$\bar{\mathbf{x}}_1: \ \bar{c}_A = c_0, \quad \bar{c}_B = 0; \quad \omega = 0 \qquad \text{(T.14.2)}$$

$$\bar{\mathbf{x}}_2: \ \bar{c}_A = 0, \quad \bar{c}_B = c_0; \quad \omega = 0 \qquad \text{(T.14.3)}$$

The system is competitive. Analysis of the higher-order terms (Fig. 44) reveals that $\bar{\mathbf{x}}_1$ is stable for $k_A > k_B$. The condition $k_A < k_B$, on the other hand, leads to stability of $\bar{\mathbf{x}}_2$.

(2) Coupling terms of fourth order:

$$\dot{c}_A = k_A c_A^2 c_B^2 - \frac{c_A}{c_0}\phi; \quad \phi = (k_A + k_B) c_A^2 c_B^2$$

$$\dot{c}_B = k_B c_A^2 c_B^2 - \frac{c_B}{c_0}\phi \quad c_0 = c_A + c_B \qquad \text{(T.14.4)}$$

This dynamic system is characterized by three fixed points:

$$\bar{\mathbf{x}}_1: \ \bar{c}_A = 0, \quad \bar{c}_B = 0; \quad \omega = 0 \qquad \text{(T.14.5)}$$

$$\bar{\mathbf{x}}_2: \ \bar{c}_A = 0, \quad \bar{c}_B = c_0; \quad \omega = 0 \qquad \text{(T.14.6)}$$

$$\bar{\mathbf{x}}_3: \ \bar{c}_A = \frac{k_A}{k_A + k_B} c_0, \quad \bar{c}_B = \frac{k_B}{k_A + k_B} c_0;$$

$$\omega = \frac{k_A^2 k_B^2}{(k_A + k_B)^3} c_0^3 \qquad \text{(T.14.7)}$$

$\bar{\mathbf{x}}_3$ thus represents a stable fixed point indicating cooperative behavior of the two coupled hypercycles H_A and H_B under all possible conditions. The vector field shown in Figure 44 reveals that the other two fixed points $\bar{\mathbf{x}}_1$ and $\bar{\mathbf{x}}_2$ are sources.

degree of freedom. As we see from Figure 44 the two hypercycles still compete despite the presence of the catalytic factors. The kind of catalytic coupling introduced, thus, was not sufficient to cause cooperative behavior.

If we increase the order of the catalytic terms by one, the dynamic system involves fourth-order growth-rate terms ($k_A c_A^2 c_B^2$, $k_B c_A^2 c_B^2$). Analyzing the vector field in the same way as before (Fig. 44), we find a stable fixed point at finite concentrations of both hypercycles (see also Table 14). Thus the quadratic coupling term is sufficient to cause cooperativity among catalytic hypercycles.

The physical realization of this type of catalytic coupling is difficult to visualize at the level of biologic macromolecules: The presence of a term like $k_A c_A^2 c_B^2$ or $k_B c_A^2 c_B^2$ in the overall rate equations requires either a complicated many-step mechanism or an encounter of more than two macromolecules, both of which are improbable*. One is tempted therefore to conclude that further development to more complex structures that consist of hierarchically coupled self-replicative units does not likely occur by introduction of higher-order catalytic terms into a system growing in homogeneous solution, but rather leads toward individualization of the already existing functional units. This can be achieved, for example, by spatial isolation of all members of a hypercycle in a compartment. Formation of prototypes of our present cells may serve as one possible mechanism leading to individualized hypercycles. After isolation is accomplished the individualized hypercycle may behave like a simple replicative unit. Hypercycles therefore are more likely to be intermediates of self-organization than final destinations.

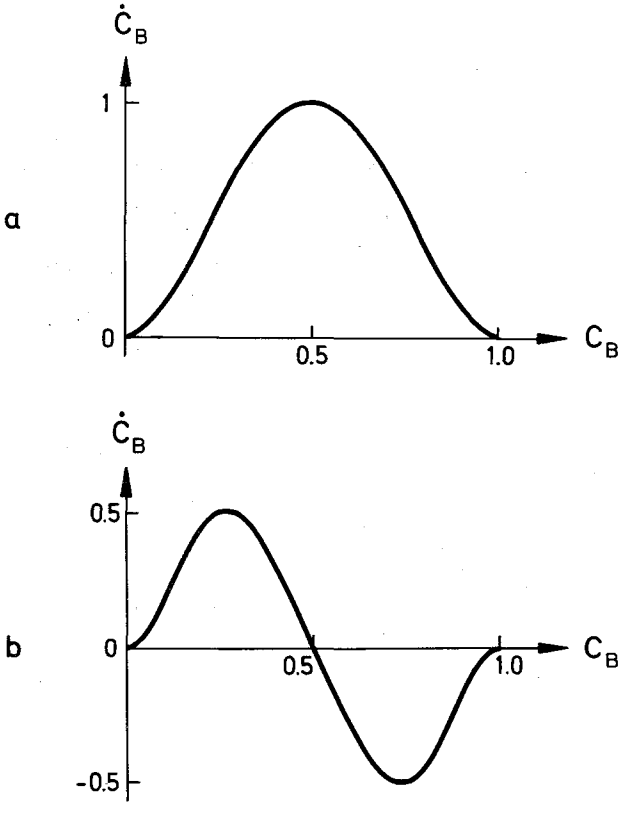

Fig. 44. Coupling between hypercycles. a) Catalytic coupling terms $k_A c_A^2 c_B$ and $k_B c_A c_B^2$, respectively. The tangent vector is positive inside the physically allowed region ($0 < c_B < 1$), except at the two fixed points; $k_B > k_A$ is assumed and consequently the hypercycle c_B is selected. The system is competitive despite the coupling term. b) Catalytic coupling terms $k_A c_A^2 c_B^2$ and $k_B c_A^2 c_B^2$, respectively. The system contains two unstable fixed points at the corners and a stable fixed point at the center ($\bar{c}_A = \bar{c}_B = 0.5$ because $k_A = k_B$). The system is cooperative

Conclusions

The main object of Part B is an abstract comparative study of various functional links in self-replicative systems. The methods used are common in differential topology. Complete analytical solutions – except in special cases – are usually not available, since the differential equations involved are inherently nonlinear. Self-reproduction always induces a dependence of production rates on population numbers of the respective species. Cooperation among different species via encoded functional linkages superimposes further concentration terms, which lead to higher-order dependences of rates on population variables.

A comparative analysis of selective and evolutive behavior does not require a knowledge of the complete solution curves. Usually it is sufficient to find their final destinations in order to decide whether or not stable coexistence of all partners of a functionally cooperative ensemble is possible. Fixed-point analysis, aided by Lyapounov's method and – in some cases – by a more detailed inspection of the complete vector field, serves the purpose quite well. The results of the combined analysis may be summarized as follows:

Functional integration of an ensemble consisting of several self-replicative units requires the introduction of catalytic links among all partners. These linkages, superimposed on the individual replication cycles of the subunits, must form a closed loop, in order to stabilize the ensemble via mutual control of all population variables. Independent competitors, which under certain spatial conditions and for limited time spans may coexist in 'niches', as well as catalytic chains or branched networks

* Artificial dynamic systems that are based on technical devices to introduce catalytic coupling terms like, e.g., electric networks may not encounter these difficulties.

are devoid of self-organizing properties, typical of hypercycles. Mere coexistence is not sufficient to yield coherent growth and evolution of all partners of an ensemble. In particular, the hypercycle is distinguished by the following properties:

1. It provides stable and controlled coexistence of all species connected via the cyclic linkage.

2. It allows for coherent growth of all its members.

3. The hypercycle competes with any single replicative unit not belonging to the cycle, irrespective of whether that entity is independent, or part of a different hypercycle, or even linked to the particular cycle by 'parasitic coupling'.

4. A hypercycle may enlarge or reduce its size, if this modification offers any selective advantage.

5. Hypercycles do not easily link up in networks of higher orders. Two hypercycles of degree p need coupling terms of degree 2p in order to stabilize each other.

6. The internal linkages and cooperative properties of a hypercycle can evolve to optimal function. 'Phenotypic' advantages, i.e., those variations which are of direct advantage to the mutant, are immediately stabilized. On the other hand, 'genotypic' advantages, which favor a subsequent product and hence only indirectly the replicative unit in which the mutation occurred, require spatial separation for competitive fixation.

7. Selection of a hypercycle is a 'once-for-ever' decision. In any common Darwinian system mutants offering a selective advantage can easily grow up and become established. Their growth properties are independent of the population size. For hypercycles, selective advantages are always functions of population numbers, due to the inherently nonlinear properties of hypercycles. Therefore a hypercycle, once established, can not easily be replaced by any newcomer, since new species always emerge as one copy (or a few).

All these properties make hypercycles a unique class of self-organizing chemical networks. This in itself justifies a more formal inspection of their properties – which has been the object of this Part B. Simple representatives of this class can be met in nature, as was shown in Part A. This type of functional organization may well be widely distributed and play some role in neural networks or in social systems. On the other hand, we do not wish to treat hypercycles as a fetish. Their role in molecular self-organization is limited. They permit an integration of information, as was required in the origin of translation. However, the hypercycle may have disappeared as soon as an enzymic machinery with high reproduction fidelity was available, to individualize the integrated system in the form of the living cell. Individualized replicative systems have a much higher potential for further diversification and differentiation.

There are many forms of hypercyclic organization ranging from straightforward second-order coupling to the nth *order compound hypercycle in which cooperative action of all members is required for each reaction step. While we do not know of any form of organization simpler than a second-order hypercycle that could initiate a translation apparatus, we are well aware of the complexity of even this 'simplest possible' system. It will therefore be our task to show in Part C that realistic hypercycles indeed can emerge from simpler precursors present in sufficient abundance under primordial conditions.*

47. Fox, S.W., in: Protein Structure and Function, p. 126 (eds. J.L. Fox, Z. Deyl, A. Blazer). New York: M. Dekker 1976
48. Hirsch, M.W., Smale, S.: Differential Equations, Dynamical Systems and Linear Algebra. New York: Academic Press 1974
49. Glansdorff, P., Prigogine, I.: Thermodynamic Theory of Structure, Stability and Fluctuations. London: Wiley Interscience 1971
50. Grümm, H.R. (ed.): Analysis and Computation of Equilibria and Regions of Stability. IIASA Conf. Proc., Vol. 8, Laxenburg 1975
51. Coddington, E.A., Levinson, N.: Theory of Ordinary Differential Equations, p. 321. New York: McGraw-Hill 1955
52. Volterra, V.: Mem. Acad. Lincei *2*, 31 (1926); Lotka, A.J.: Elements of Mathematical Biology. New York: Dover 1956
53. Eigen, M., et al.: forthcoming paper
54. Schuster, P., Sigmund, K., Wolff, R.: Bull. Math. Biol. (in press)
55. Schuster, P.: Chemie in uns. Zeit *6*, 1 (1972); Schuster, P., in: Biophysik, ein Lehrbuch, p. 688. (W. Hoppe, et al., eds.). Berlin: Springer 1977
56. Bhat, R.K., Schneider, F.W.: Ber. Bunseges. physik. Chem. *80*, 1153 (1976)
57. La Salle, J., Lefschetz, S.: Stability by Lyapunov's Direct Method with Applications. New York: Academic Press 1961
58. Marsden, J.E., McCracken, M. (eds.): The Hopf Bifurcation and its Applications (Appl. Math. Sci., Vol. 19). New York: Springer 1976
59. Thom, R.: Stabilité Structurelle et Morphogenèse. New York: Benjamin 1972

Received October 27, 1977